Zoosyst. Evol. 102 (1) 2026, 159–179 | DOI 10.3897/zse.102.165834

PENSOFT

MUSEUM FÜR NATURKUNDE BERLIN

Phylogenetic classification of poorly known *Crassignatha* spiders (Araneae, Symphytognathidae), with descriptions of four new species

Haihong Wu[1,2], Yucheng Lin[1,2]

1 *Key Laboratory of Bio-resources and Eco-environment (Ministry of Education), College of Life Sciences, Sichuan University, Chengdu, Sichuan 610064, China*

2 *The Sichuan Key Laboratory for Conservation Biology of Endangered Wildlife, Sichuan University, Chengdu, Sichuan 610064, China*

https://zoobank.org/D5F53FDD-3B89-4E36-B650-124E2F6D18D6

Corresponding author: Yucheng Lin (linyucheng@scu.edu.cn)

Academic editor: Danilo Harms ♦ **Received** 21 July 2025 ♦ **Accepted** 22 December 2025 ♦ **Published** 23 January 2026

Abstract

The genus *Crassignatha* Wunderlich, 1995, represents the second most species-rich lineage within the spider family Symphytognathidae. Members of the genus are predominantly distributed in southwestern China and Southeast Asia, with the exception of *C. kishidai* (Shinkai, 2009), which is recorded from Japan. Historically, the circumscription and diagnosis of *Crassignatha* have remained ambiguous, and its monophyly has not yet been rigorously tested. In this study, we conducted a molecular phylogenetic analysis based on sequence data from five genetic markers (16S, 18S, 28S, H3, and a fragment of COI) to evaluate the monophyletic status of the genus. Sequences were obtained from 21 species of *Crassignatha* (ingroup), along with two species of *Kirinua* Li & Lin, 2021, and one species of *Patu* Marples, 1951, as the outgroup. The results support the monophyly of *Crassignatha* and confirm the taxonomic validity of the 21 included species. Five species of *Crassignatha* belonging to Symphytognathidae are reported from the Yunnan–Guizhou Plateau, four of which are newly described: *C. hekou* Wu & Lin, **sp. nov.** (♂♀), *C. qingxu* Wu & Lin, **sp. nov.** (♂♀), *C. liangdu* Wu & Lin, **sp. nov.** (♂♀), and *C. panlong* Wu & Lin, **sp. nov.** (♂♀). Additionally, a new distribution record outside the type locality is provided for the previously known species *C. shunani* Lin & S. Q. Li, 2020 (♂♀). Detailed diagnoses, descriptions, and illustrations are provided for all newly described species. The geographic distribution of *Crassignatha* is also discussed.

Key Words

Crassignatha, monophyly, new taxa, Symphytognathidae, Yunnan-Guizhou Plateau

Introduction

Symphytognathidae Hickman, 1931 is a relatively poorly studied family of spiders characterized by their extremely small size (adult body length ca. 1 mm or less). It currently comprises 10 extant genera and 108 described species (Brescovit and Cizauskas 2025; WSC 2025), with no fossil representatives known to date (Dunlop et al. 2023). Notably, this family includes the world's smallest described adult spider, *Patu digua* Forster & Platnick, 1977, which measures approximately 0.33 mm in body length (Mammola et al. 2017). Members of this family are broadly distributed across all continents and some oceanic islands, excluding Antarctica. Their diversity is particularly high in the tropical and subtropical regions of the Oriental and Neotropical realms. These minute spiders typically occupy cryptic microhabitats such as forest leaf litter, soil crevices, and accumulations of debris near cave entrances (Cardoso and Scharff 2009; Lin and Li 2009; Miller et al. 2014).

Crassignatha Wunderlich, 1995, was originally established as a monotypic genus and placed by Wunderlich (1986) within the subfamily Synaphrinae Wunderlich, 1986, which was then considered part of Anapidae (*sensu lato*). Subsequent taxonomic treatments reflected ongoing uncertainty regarding its familial placement.

Copyright *Wu, H. & Lin, Y.* This is an open access article distributed under the terms of the Creative Commons Attribution License (CC BY 4.0), which permits unrestricted use, distribution, and reproduction in any medium, provided the original author and source are credited.

Marusik and Lehtinen (2003) later suggested a possible affinity with Symphytognathidae Hickman, 1931, a view contested by Wunderlich (2004), who retained its classification within Anapidae (*sensu stricto*). Platnick (2008) subsequently catalogued this genus under Mysmenidae Petrunkevith, 1928. A shift in consensus began with Miller et al. (2009), who formally transferred *Crassignatha* to Symphytognathidae based on distinct morphological similarities shared with certain species of *Patu* Marples, 1951. This period was characterized by broader systematic ambiguity surrounding the delimitation of symphytognathoid families, particularly Anapidae, Mysmenidae, and Symphytognathidae. The systematic position of *Crassignatha* was not conclusively resolved until the phylogenetic study by Lopardo and Hormiga (2015), which robustly confirmed its placement within Symphytognathida.

Since its establishment three decades ago, *Crassignatha* has expanded from a monotypic genus into the second most species-rich genus in Symphytognathidae. To date, it comprises 28 described species, the vast majority of which are distributed in South China (south of the Yangtze River) and the Indochinese Peninsula (Miller et al. 2009; Miller et al. 2014; Li et al. 2020; Li et al. 2021; Rivera-Quiroz et al. 2021). A notable exception is *Crassignatha kishidai*, which is known only from central and southern Japan (Shinkai 2009). Nevertheless, the biogeographic patterns underlying this distribution have not been explicitly addressed in previous studies. Furthermore, the taxonomic validity and phylogenetic relationships among the constituent species remain inadequately tested and require systematic confirmation.

During recent field surveys of karst cave systems on the Yunnan-Guizhou Plateau, numerous micro-spider specimens were collected. This study provides a systematic taxonomic treatment of this material, leading to the recognition of four new species of *Crassignatha*, together with new locality records for one previously described species. The specific objectives are to (1) describe four novel *Crassignatha* species from the Yunnan-Guizhou Plateau, thereby expanding the known diversity of the genus; (2) generate and present multi-locus molecular data for both new and known *Crassignatha* species to strengthen their taxonomic characterization; (3) assess the monophyly of *Crassignatha* using phylogenetic methods; and (4) analyze the geographical distribution range and patterns exhibited by this genus.

Materials and methods

Morphological data

All specimens were manually collected during field surveys and preserved immediately in 95% ethanol. The examined morphological material and associated molecular vouchers are deposited in the Natural History Museum of Sichuan University, Chengdu, China (**NHMSU**).

Specimens were examined using a Leica M205 C stereomicroscope. Morphological imaging was performed using a Canon EOS 60D digital camera (8.5 megapixels) mounted on an Olympus BX43 compound microscope. For detailed morphological examination, male palps and female epigynes were carefully dissected prior to observation. The left palp was photographed in most cases, with the right palp used when necessary. Epigynes were cleared in lactic acid and subsequently mounted in Hoyer's medium on ultra-thin slides to facilitate bilateral observation of the vulval structures. All images were stacked using Helicon Focus 3.10 software (Khmelik et al. 2006) and processed in Adobe Photoshop 7.0 software. Measurements are given in millimeters. Leg segment lengths are listed in the standard order: femur, patella, tibia, metatarsus, and tarsus. Morphological abbreviations used in the text and figures are explained in Table 1. Illustrations are referred to following standard scientific format (Fig. and Figs or fig. and figs).

Table 1. List of abbreviations used in the text or figures.

ALE	anterior lateral eye	**MA**	median apophysis
AS	abdominal scutum in male	**Pa**	patella
CD	copulatory duct	**PER**	posterior eye row
CO	copulatory opening	**PLE**	posterior lateral eye
CT	cymbial tooth	**PME**	posterior median eye
Cy	cymbium	**S**	spermatheca
E	embolus	**Sp**	scape
ED	ejaculatory duct	**T**	tegulum
EM	embolic membrane	**Ti**	tibia
FD	fertilization ducts	**TS**	tibial spur on leg II in male

Molecular data

Genomic DNA was extracted from specimens representing 21 *Crassignatha* species and three outgroup species (Table 3). For molecular analyses, the prosoma and legs were used, whereas the remaining opisthosoma and male palps were preserved as voucher material for subsequent morphological verification. Five molecular markers were amplified and sequenced: the mitochondrial 16S rRNA and cytochrome c oxidase subunit I (COI) genes and the nuclear 18S rRNA, 28S rRNA, and histone H3 genes. Primer sequences used in this study are listed in Table 2. The phylogenetic dataset was compiled from (1) novel sequences generated in this study and (2) previously published sequences from representative taxa. This resulted in a matrix of 24 terminal taxa, including 21 ingroup taxa (17 described *Crassignatha* species and four new species) and three outgroup taxa (one *Kirinua* species and two *Patu* species; see Table 3). Genetic distances between species were calculated using MEGA 12.0.0 (Kumar et al. 2024), with the results presented in Suppl. material 1.

Sequences were edited and assembled using Chromas software. Multiple sequence alignment was performed

Table 2. Primers used in PCR in this study.

Locus	Primer	OR	Sequence 5→3 (forward and reverse)	Reference
18S	18s_1F	F	TACCTGGTTGATCCTGCCAGTAG	(Giribet et al. 1996)
	18S_1000R	R	GTGGTGCCCTTCCGTCAATT	(Balczun et al. 2005)
28S	28sa	F	GACCCGTCTTGAAACACGGA	(Rix et al. 2008)
	LSUR	R	GCTACTACCACCAAGATCTGCA	
H3	H3af	F	ATGGCTCGTACCAAGCAGACVGC	(Colgan et al. 1998)
	H3ar	R	ATATCCTTRGGCATRATRGTGAC	
	H3nf-	F	ATGGCTCGTACCAAGCAGAC	
	H3nr	R	ATRTCCTTGGGCATGATTGTTAC	
CO1	LCO1490	F	GGTCAACAAATCATAAAGATATTGG	(Simon et al. 1994)
	CO1-Nancy	R	CCCGGTAAAATTAAAATATAAACTTC	
16S	16sb2_12864	F	CTCCGGTTTGAACTCAGATCA	(Hormiga et al. 2003)
	LR-J-13360	R	GTAAGGCCTGCTCAATGA	(Zhang and Lin 2023)
	16S-A	F	CGCCTGTTTATCAAAAACAT	(Palumbi et al. 1991)
	16S-B	R	CTCCGGTTTGAACTCAGATCA	

using MAFFT v.7.450 (Katoh and Standley 2013) via its online server (https://mafft.cbrc.jp/alignment/server/). Phylogenetic analyses were conducted on a concatenated dataset of five molecular markers (16S, COI, 18S, 28S, and H3) using maximum likelihood (ML) and Bayesian inference (BI) approaches. The ML analysis was performed using IQ-TREE v1.6.9 (Nguyen et al. 2015) implemented in PhyloSuite v1.2.2 (Zhang et al. 2020), employing 2,000 ultrafast bootstrap replicates with TBR branch swapping. The BI analysis was conducted using MrBayes v3.1.2 (Ronquist et al. 2012) on the CIPRES Science Gateway. Two independent runs, each consisting of four Markov chain Monte Carlo (MCMC) chains, were executed for 50 million generations, with trees sampled every 1,000 generations. The first 25% of the sampled trees were discarded as burn-in after confirming that the average standard deviation of split frequencies had fallen below 0.01. Convergence of the MCMC runs was assessed using Tracer v1.7.1 (Rambaut et al. 2018). All phylogenetic computations were coordinated through the PhyloSuite v1.2.2 platform. The resulting phylogenetic tree was visualized and annotated using the Interactive Tree of Life (iTOL) platform (Letunic and Bork 2021).

Geobiological data

Distribution records for the target taxa were derived from two sources: original field investigations conducted during this study and a compilation of locality data extracted from published literatures. For each species, geographic coordinates (latitude and longitude) were recorded and compiled into a unified dataset. All coordinates were georeferenced and mapped using ArcGIS 10.8 Esri 2020) to generate a species distribution map (Fig. 13). To visualize phylogenetic–geographic relationships, distribution points on the map were color-coded and numbered sequentially according to the phylogenetic position of the corresponding species (Figs 1, 2), with each number representing a distinct species.

Results

Phylogenetic analysis

Phylogenetic analyses of the concatenated dataset comprising five molecular markers produced highly concordant topologies under ML and BI frameworks (Figs 1, 2). All terminal clades were strongly supported (ML bootstrap ≥ 90%; BI posterior probability ≥ 0.95). The analyses robustly resolved evolutionary relationships among *Crassignatha* species and clarified their position relative to the closely related genera *Kirinua* and *Patu*. *Crassignatha* was recovered as a maximally supported monophyletic group (ML = 100%; PP = 1.0) and formed a sister clade to the outgroup taxa comprising *Kirinua* and *Patu*.

The ML phylogeny revealed clear evolutionary structuring within *Crassignatha* (Fig. 1). Four previously described species—*C. shiluensis*, *C. shunani*, *C. nantou*, and *C. nasalis*—were resolved in strongly supported basal positions (bootstrap ≥ 90%), consistent with early divergence and the retention of plesiomorphic traits. The newly described *C. qingxu* sp. nov. occupied an intermediate phylogenetic position between these basal lineages and the more derived clades. The remaining 16 species clustered into four well-supported clades: (1) a strongly supported monophyletic group (bootstrap = 95%) containing *C. hekou* sp. nov. and *C. ertou*; (2) a robust subclade (bootstrap = 98%) comprising *C. liangdu* sp. nov. and *C. panlong* sp. nov., within which *C. liangdu* sp. nov. formed a maximally supported terminal branch with *C. si* (bootstrap = 100%), corroborating their shared morphological synapomorphies; (3) a moderately supported lineage (bootstrap = 75%) grouping *C. dongnai*, *C. mengla*, *C. quadriventris*, and *C. baihua*; and (4) a distinct clade (bootstrap = 92%) consisting of *C. gucheng*, *C. thamphra*, *C. bangbie*, and *C. rostriformis*. These phylogenetic groupings are strongly congruent with the morphological distinctions observed among the species.

The BI phylogeny was fully congruent with the ML topology across all major clades (Fig. 2), with strong

Table 3. List of 24 species of *Crassignatha*, *Kirinua* and *Patu* and their DNA data used for molecular phyligenetic analysis (new sequences marked with "*" obtained in this study).

Species	Identifer	Ses/Stage	16S*	18S*	28S*	COI	H3*
Crassignatha baihua	HA109	♂/adult	PX776304	PX766943	PX832576	MT992007	PX900800
	HA109	♀/adult	PX776303	PX766942	PX832575	MT992006	PX900799
Crassignatha bangbie	HA137	♀/adult	PX776305	PX766944	PX832577	MT992015	PX900801
Crassignatha dongnai	HA092	♀/adult	PX776306	PX766945	PX832578	MT992004	PX900802
Crassignatha ertou	HA108	♀/adult	—	PX766946	PX832579	MT992005	PX900803
Crassignatha gucheng	HA132	♀/adult	PX776307	PX766947	PX832580	MT992014	PX900804
Crassignatha hekou **sp. nov.**	YG160	♂/adult	—	PX766935	PX832604	PX830427*	PX900807
	YG160	♀/adult	—	PX766934	PX832603	PX830426*	PX900806
Crassignatha liangdu **sp. nov.**	YG166	♂/adult	PX776297	PX766937	PX832606	PX830429*	PX900809
	YG166	♀/adult	PX776298	PX766936	PX832605	PX830428*	PX900808
Crassignatha mengla	HA080	♂/juvenile	PX776309	PX766949	PX832582	MT992000	PX900811
	HA080	♀/adult	PX776308	PX766948	PX832581	MT991999	PX900810
Crassignatha nantou	HA055	♂/adult	PX776311	PX766951	PX832584	MT991996	PX900813
	HA055	♀/adult	PX776310	PX766950	PX832583	MT991995	PX900812
Crassignatha nasalis	HA041	♂/adult	PX776313	PX766953	PX832586	MT991992	PX900815
	HA041	♀/adult	PX776312	PX766952	PX832585	MT991991	PX900814
Crassignatha panlong **sp. nov.**	YG162	♂/adult	PX776299	PX766939	PX832608	PX830431*	PX900817
	YG162	♀/adult	PX776300	PX766938	PX832607	PX830430*	PX900816
Crassignatha pianma	HA113	♂/adult	PX776315	PX766955	PX832588	MT992009	PX900819
	HA113	♀/adult	PX776314	PX766954	PX832587	MT992008	PX900818
Crassignatha qingxu **sp. nov.**	YG170	♂/adult	PX776302	PX766941	PX832609	PX830433*	PX900821
	YG170	♀/adult	PX776301	PX766940	PX832610	PX830432*	PX900820
Crassignatha quadriventris	HA025	♀/adult	PX776316	PX766956	PX832589	MT991990	PX900822
Crassignatha rostriformis	HA079	♂/adult	PX776318	PX766958	PX832591	MT991998	PX900824
	HA079	♀/adult	PX776317	PX766957	PX832590	MT991997	PX900823
Crassignatha shiluensis	HA081	♂/juvenile	PX776320	—	PX832593	MT992002	—
	HA081	♀/adult	PX776319	PX766959	PX832592	MT992001	PX900825
Crassignatha shunani	HA046	♂/juvenile	PX776322	PX766960	PX832595	MT991994	PX900827
	HA046	♀/adult	PX776321	PX766961	PX832594	MT991993	PX900826
Crassignatha si	HA141	♂/juvenile	PX776324	PX766963	PX832597	MT992017	PX900829
	HA141	♀/juvenile	PX776323	PX766962	PX832596	MT992016	PX900828
Crassignatha thamphra	HA089	♀/adult	PX776325	PX766964	PX832598	MT992003	PX900830
Crassignatha yamu	HA115	♂/adult	PX776327	PX766966	PX832600	MT992011	PX900832
	HA115	♀/adult	PX776326	PX766965	PX832599	MT992010	PX900831
Crassignatha yinzhi	HA117	♂/adult	PX776329	PX766968	PX832602	MT992013	PX900834
	HA117	♀/adult	PX776328	PX766967	PX832601	MT992012	PX900833
Kirinua yangshuo	HA018	♂/juvenile	PX776335	PX766970	PX832570	MW970236	PX900836
	HA018	♀/adult	PX776334	PX766969	PX832569	MW970235	PX900835
Patu xiaoxiao	HA123	♂/adult	PX776333	PX766974	PX832574	MW970245	PX900840
	HA123	♀/adult	PX776332	PX766973	PX832573	MW970244	PX900839
Patu jidanweishi	HA119	♂/adult	PX776331	PX766972	PX832572	MW970243	PX900838
	HA119	♀/adult	PX776330	PX766971	PX832571	MW970242	PX900837

nodal support for all terminal branches (posterior probabilities ≥ 0.95). This high degree of concordance between independent analytical methods robustly supports (1) the taxonomic validity of the four newly described *Crassignatha* species, (2) the substantial phylogenetic divergence present within the genus, and (3) the monophyly of *Crassignatha* (PP = 1.0).

The strong concordance between the independent ML and BI analyses provides robust validation of (a) the species-level distinctness of the four newly proposed taxa, (b) the current systematic classification of *Crassignatha*, and (c) the effectiveness of the molecular markers employed for resolving phylogenetic relationships within this genus. These results establish a reliable phylogenetic framework for future taxonomic studies and underscore the importance of continued molecular characterization of poorly studied *Crassignatha* lineages.

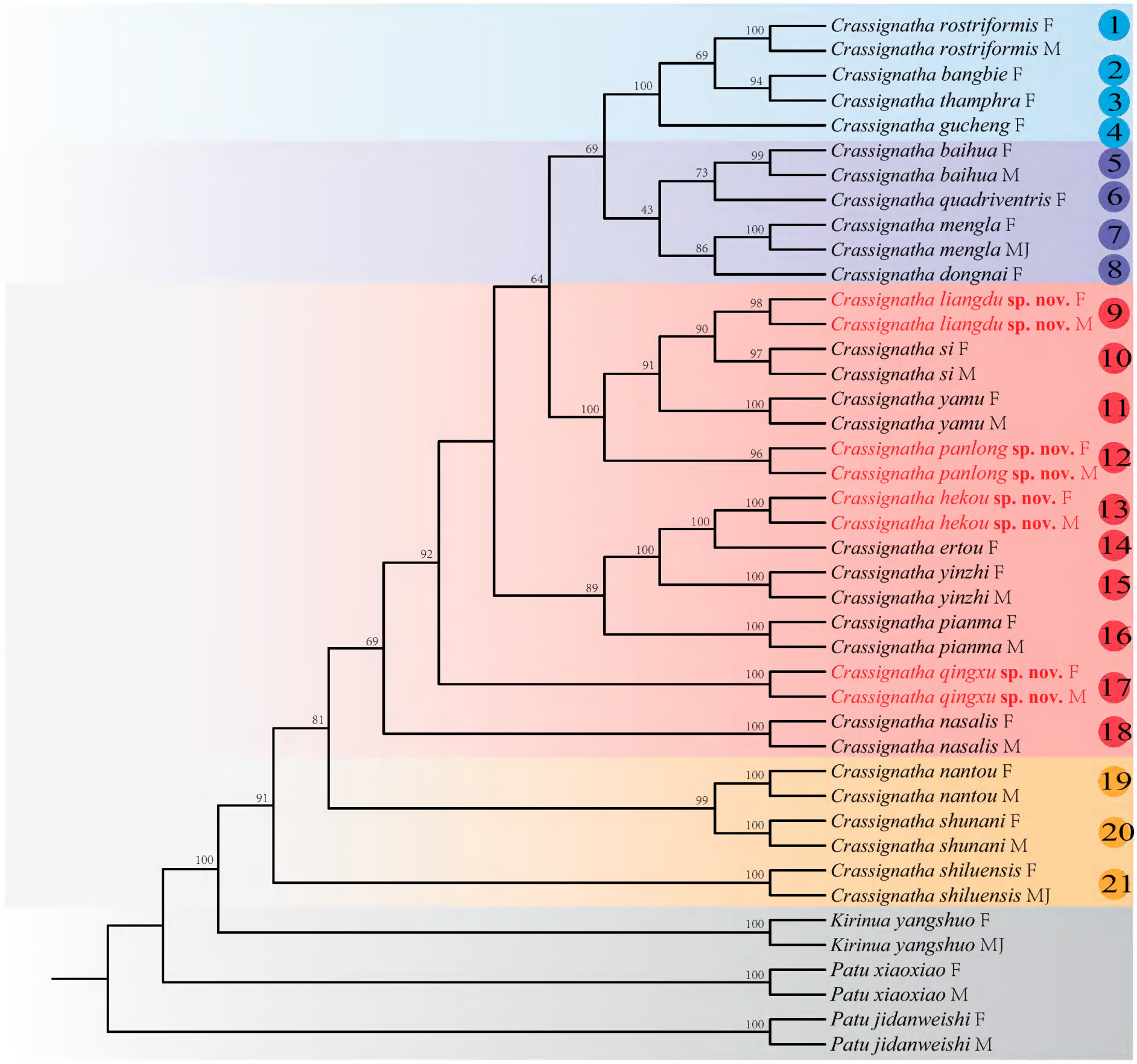

Figure 1. Tree topology obtained using maximum likelihood analysis in IQ-TREE v2.0. Numbers at nodes indicate bootstrap values. Twenty-one species representing the genus *Crassignatha* cluster together to form a monophyletic clade with high support (yellow, red, blue, and purple boxes). Numbering and branch colors correspond to those used in Fig. 13. Species within the gray box represent the outgroup. Red text indicates newly described species.

Taxonomy

Family Symphytognathidae Hickman, 1931

Genus *Crassignatha* Wunderlich, 1995

Crassignatha Wunderlich, 1995: 546; Miller et al. 2009: 68; Li et al. 2020: 66.

Type species. *Crassignatha haeneli* Wunderlich, 1995, by original designation, from Malaysia.

Diagnosis and description. See Li et al. 2020: 66–67 in detail.

Composition. *Crassignatha baihua* Lin & Li, 2020 (♂♀), *C. bangbie* Lin & Li, 2020 (♂♀), *C. bicorniventris* (Lin & Li, 2009) (♀), *C. bispina* (Lin, Pham & Li, 2009) (♂♀), *C. changyan* Lin & Li, 2020 (♀), *C. danaugirangensis* Miller et al., 2014 (♂♀), *C. dongnai* Lin & Li, 2020 (♀), *C. ertou* Miller, Griswold & Yin, 2009 (♂♀), *C. gucheng* Lin & Li, 2020 (♂♀), *C. gudu* Miller, Griswold & Yin, 2009 (♀), *C. haeneli* Wunderlich, 1995 (♂), *C. hekou* Wu & Lin, sp. nov. (♂♀), *C. kishidai* (Shinkai, 2009) (♂♀), *C. liangdu* Wu & Lin, sp. nov. (♂♀), *C. mengla* Lin & Li, 2020 (♂♀), *C. nantou* Lin & Li, 2020 (♂♀), *C. nasalis* Lin & Li, 2020 (♂♀), *C. panlong* Wu & Lin, sp. nov. (♂♀), *C. pianma* Miller, Griswold & Yin, 2009 (♂♀), *C. qingxu* Wu & Lin, sp. nov. (♂♀), *C. quadriventris* (Lin & Li, 2009) (♂♀), *C. quanqu* Miller, Griswold & Yin, 2009 (♂♀), *C. rostriformis* Lin & Li, 2020 (♂♀), *C. seedam* Rivera-Quiroz, Petcharad & Miller, 2021 (♀), *C. seeliam* Rivera-Quiroz, Petcharad & Miller, 2021 (♂♀),

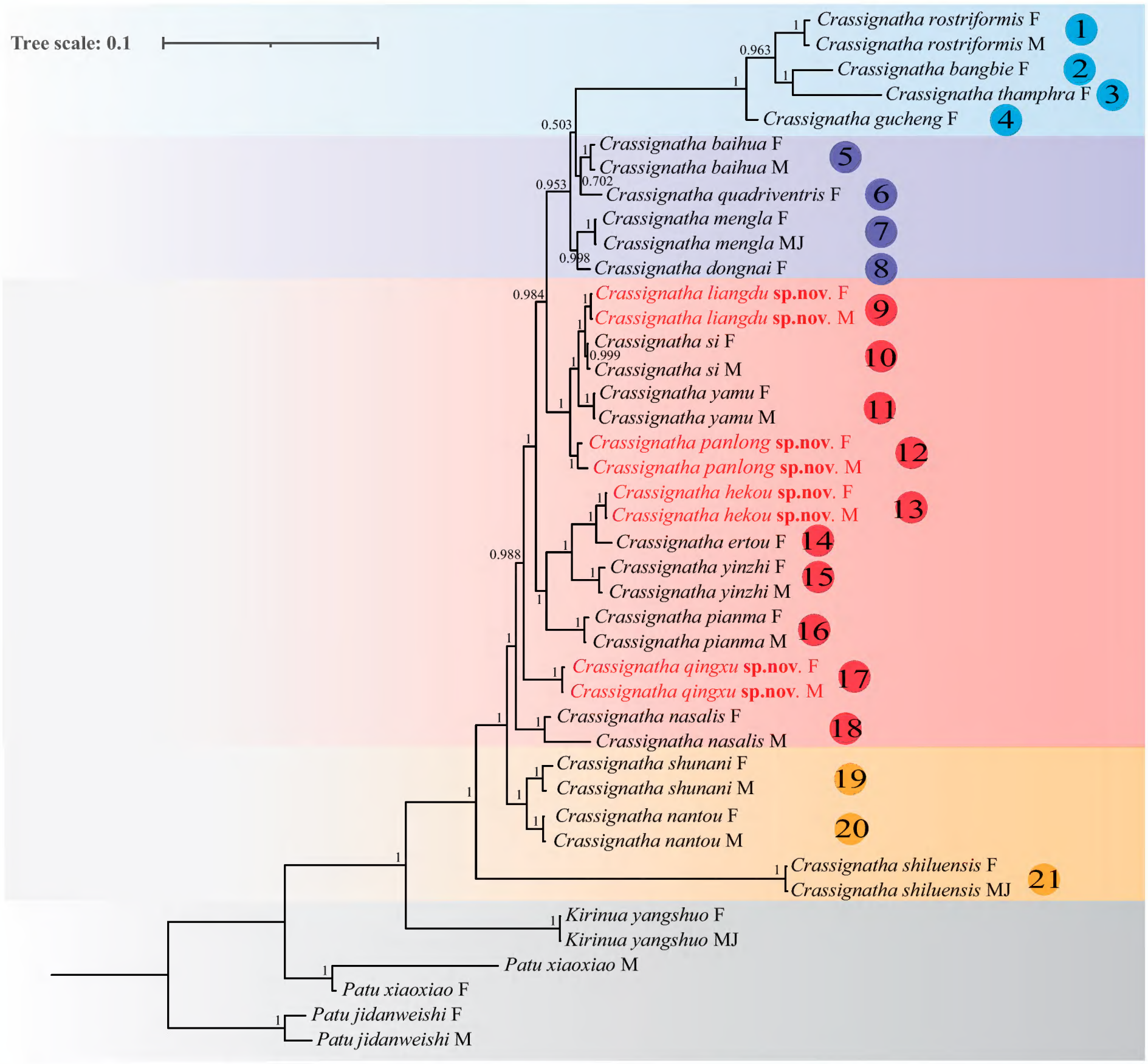

Figure 2. Tree topology obtained from Bayesian inference analysis in MrBayes v3.2.7. Numbers at nodes indicate posterior probabilities. Other settings and annotations are the same as in Fig. 1. The phylogenetic tree constructed using the Bayesian method supports the monophyly of the four newly described species.

C. shiluensis (Lin & Li, 2009) (♂♀), *C. shunani* Lin & Li, 2020 (♂♀), *C. si* Lin & Li, 2020 (♂♀), *C. thamphra* Lin & Li, 2020 (♀), *C. xichou* Lin & Li, 2020 (♀), *C. yamu* Miller, Griswold & Yin, 2009 (♂♀), and *C. yinzhi* Miller, Griswold & Yin, 2009 (♂♀).

Distribution. Southern China (Guizhou, Yunnan, Hainan, and Taiwan), Central Japan (Honshu, Shikoku), Vietnam, Thailand, and Malaysia.

Comments. The spider genus *Crassignatha* was initially placed in Synaphridae (Wunderlich 1995), later cataloged within Mysmenidae (WSC 2025), and subsequently transferred to Symphytognathidae, where it is currently classified (Miller et al. 2009; Lopardo and Hormiga 2015; Li et al. 2020). The genus now comprises 32 species, including the four newly described in this study, and is primarily distributed across the Far East and Southeast Asia. With this updated species count, *Crassignatha* surpasses both *Symphytognatha* Hickman, 1931, and *Patu* Marples, 1951, in species richness, making it the second-largest genus in Symphytognathidae. It is currently exceeded only by *Anapistula* Gertsch, 1941, which contains 34 recorded species (Brescovit and Cizauskas 2025). Furthermore, *Crassignatha* represents the most species-rich genus of Symphytognathidae known from China to date.

Crassignatha hekou Wu & Lin, sp. nov.

https://zoobank.org/4BCAFF10-7E29-4425-9EFC-0355069508EA

Figs 3, 4, 13

Type material. ***Holotype*** • ♂ (NHMSU Ar 132) and ***paratypes*** • 5♂ 10♀ (NHMSU Ar 133–147), **China:** Yunnan Prov., Xundian Co., Hekou TWP., the entrance

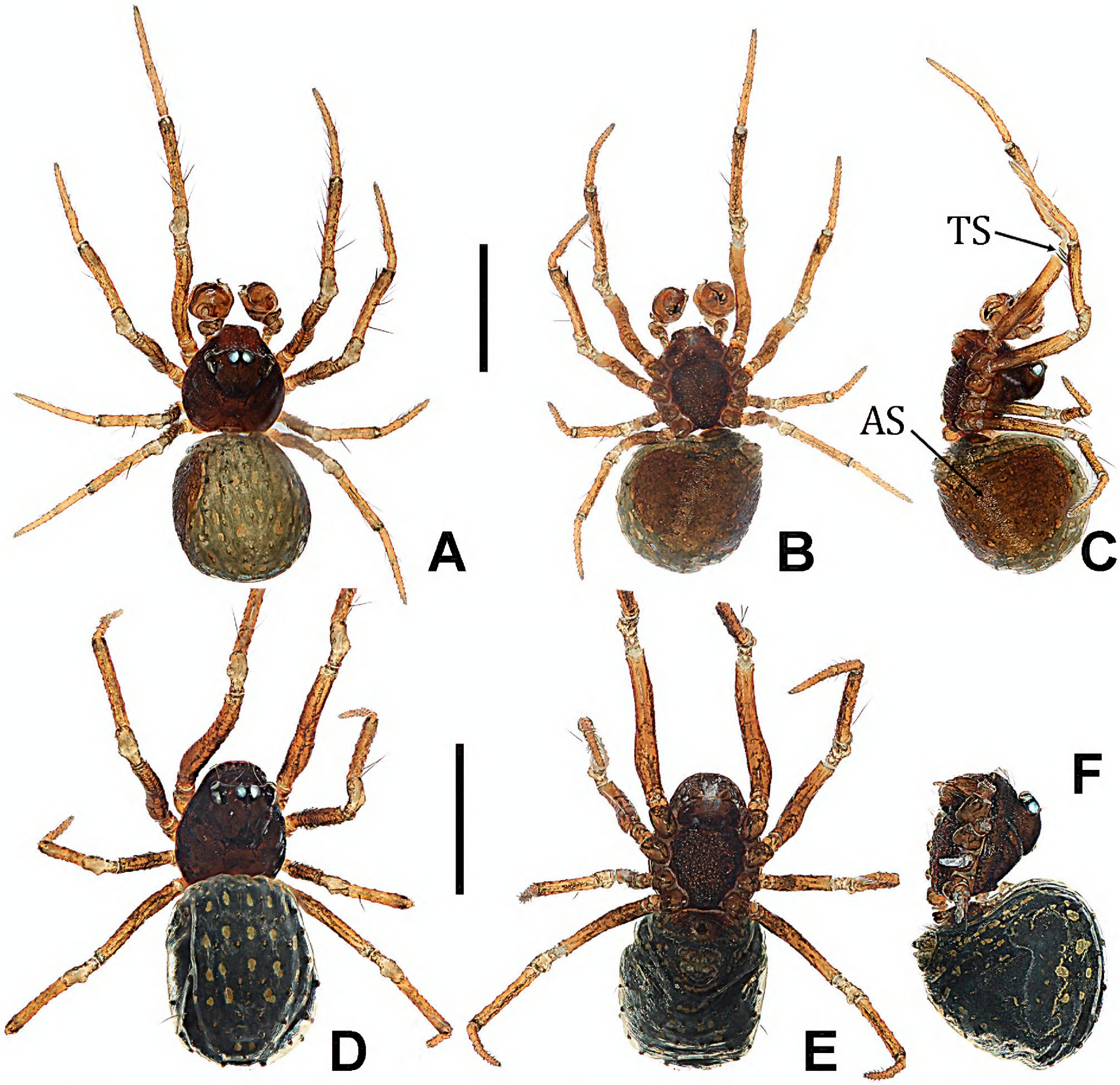

Figure 3. *Crassignatha hekou* Wu & Lin, sp. nov. **A.** Male habitus, dorsal view; **B.** Ditto, ventral view; **C.** Ditto, lateral view; **D.** Female habitus, dorsal view; **E.** Ditto, ventral view; **F.** Ditto, lateral view. Scale bars: 0.50 mm (**A–F**).

to Baishiyan Cave (25.820941°N, 103.502352°E; elev. 1863 m), 28.VIII.2020, Y. Lin, Y Li, S. Liu and Y. He leg. 1♂ (NHMSU-YG160) and 1♀ (NHMSU-YG160) used for sequencing, same data as for preceding.

Etymology. The specific epithet derives from the name of the type locality; noun in apposition.

Diagnosis. The male of *Crassignatha hekou* sp. nov. resembles those of *C. yinzhi* and *C. ertou* but can be distinguished by the presence of three TS on leg II, compared to two in *C. yinzhi* and one in *C. ertou* (cf. Fig. 3F; Li et al. 2020: figs 7C, 36C). A further distinction lies in the male pale: the embolus is straight and relatively long, whereas it is helical in *C. ertou* and is longer in *C. yinzhi* (cf. Fig. 4A–C; Li et al. 2020: figs 8A–C, 37A–C). The female of *C. hekou* sp. nov. shares a generally similar vulval configuration with *C. quanqu* but differs in possessing a longer scape and the copulatory duct with longer trajectory (cf. Fig. 4F, G; Li et al. 2020: fig. 23D, E).

Description. Male (holotype). Total length 0.87. Carapace 0.40 long, 0.36 wide, 0.40 high. Clypeus 0.12 high. Sternum 0.28 long, 0.32 wide. Abdomen 0.50 long, 0.52 wide, 0.61 high. Length of legs: I 1.50 (0.46, 0.13, 0.35, 0.22, 0.34); II 1.25 (0.37, 0.14, 0.30, 0.17, 0.27); III 0.99 (0.28, 0.11, 0.20, 0.15, 0.25); IV 1.09 (0.36, 0.13, 0.25, 0.12, 0.23).

Somatic characters (Fig. 3A–C). Prosoma dark brown. Opisthosoma grayish-brown, scattered with dot-like weakly ossified speckles, with a light brown scutum laterally and posteriorly. Carapace pear-shaped, surface granular, with rough texture. Cephalic region raised. PER recurved. ALE slightly protruded. Mouthparts sclerotized. Sternum scutiform, surface rough, with soft bristles. Legs light brown, covered with setae and bristles. Tibia II with

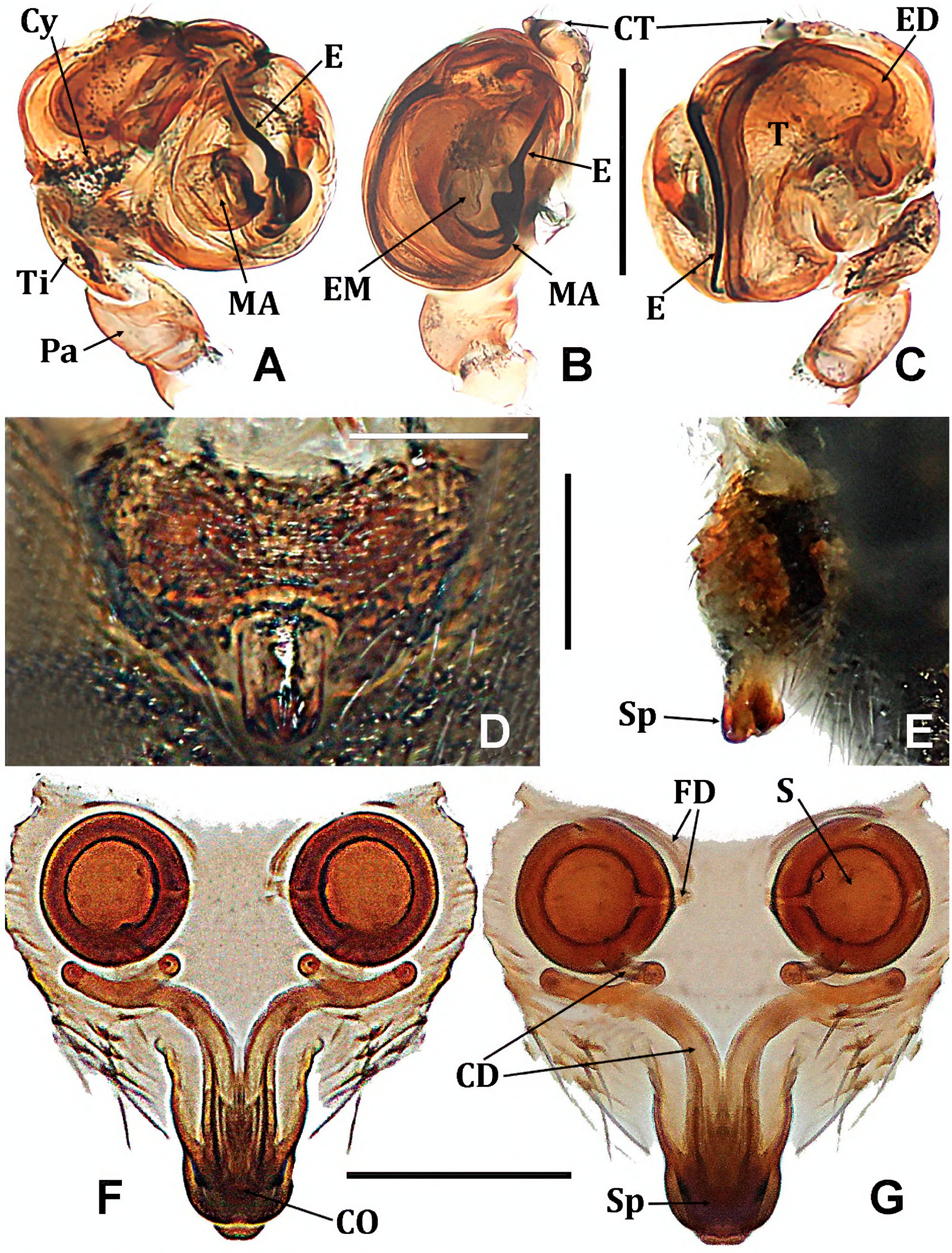

Figure 4. *Crassignatha hekou* Wu & Lin, sp. nov. **A.** Male palp, prolateral view; **B.** Ditto, ventral view; **C.** Ditto, retrolateral view; **D.** Epigyne, ventral view; **E.** Ditto, lateral view; **F.** Vulva, dorsal view; **G.** Ditto, ventral view. Scale bars: 0.10 mm (**A–G**).

three disto-ventral clasping spurs. Opisthosoma dorsally rounded, laterally near triangular. Abdominal scutum almost covers lateral and posterior areas. Spinnerets light brown, surrounded by a circular shield.

Palp (Fig. 4A–C): bulb relatively large, each ~¼ size of carapace. Tibia same long as patella. Cymbium wraps the bulb on prolaterally, bears apical short setea, cymbial tooth short, nail-shaped. Bulb compressed, smooth on

retrolaterally. Tegulum smooth, bulgy. Median apophysis oblate, nearly square, with a distal process. Embolic membrane translucent, arises between embolus and median apophysis. Embolus nearly straight, strongly sclerotized, wide base slightly curved, gradually tapering on medially and distally.

Female (one of paratypes). Total length 1.00. Carapace 0.48 long, 0.40 wide, 0.35 high. Clypeus 0.12 high. Sternum 0.32 long, 0.24 wide. Abdomen 0.60 long, 0.48 wide, 0.70 high. Length of legs: I 1.68 (0.59, 0.16, 0.40, 0.24, 0.29); II 1.36 (0.43, 0.15, 0.34, 0.20, 0.24); III 0.96 (0.31, 0.10, 0.19, 0.15, 0.21); IV 1.25 (0.42, 0.13, 0.30, 0.17, 0.23).

Somatic characters. (Fig. 3D–F). Prosoma and opisthosoma darker than in male. Abdominal scutum unobvious. Leg II lacks clasping spurs on tibia disto-ventrally.

Epigyne (Fig. 4D–G): Epigynal area obvious sclerotized, covered sparse setae, chitin epidermis wrinkled. Scape protruded, extends beyond the epigastric furrow, longer than wide, distally sclerotized. Spermatheca nearly globular, spacing by ~¾× their diameter. Fertilization ducts short and gracile, starting at inner-ventral side of spermathecae. Copulatory ducts long, uniform width, weakly sclerotized, connected to dorso-posterior surface of spermathecae, forming three turns before curving downward. Subproximal copulatory ducts nearly parallel, opening at the end of scape.

Distribution. China (Yunnan).

***Crassignatha liangdu* Wu & Lin, sp. nov.**

https://zoobank.org/51FF5629-1839-4EC6-9480-F601DA21B01E

Figs 5, 6, 13

Type material. ***Holotype*** • ♂ (NHMSU Ar 148) and ***paratypes*** • 2♂ 7♀ (NHMSU Ar 149–155), **China:** Guizhou Prov., Liupanshui Ct., Panzhou county-level Ct., Zhudong TWP, Shiliping Vill., nr. Shilida Cave (25.623685°N, 104.756623°E; elev. 1658 m), 24.VIII.2020, Y. Lin et al. leg. 1♂ (NHMSU-YG166) and 1♀ (NHMSU-YG166) used for sequencing, same data as for preceding.

Other material examined. • 1♂ 3♀ (NHMSU Ar 156–159), **China:** Guizhou Prov., Liupanshui Ct., Panzhou county-level Ct., the entrance to Zimu Cave on Danxia Hill (25.675198°N, 104.626882°E; elev. 1791 m), 24.VIII.2020, Y. Lin, Y. Li and S. Liu leg. • 1♂ 14♀ (NHMSU Ar 160–174), **China:** Yunnan Prov., Kunming Ct., Xishan Distr., Tuanjie TWS., Qingshuiguan Vill., nr. Guanyin Cave (25.192443°N, 102.791204°E; elev. 2159 m), 27.VIII.2020, Y. Lin, Y. Li and S. Liu leg.

Etymology. The specific epithet derives from a Chinese pinyin for "Liangdu", meaning is a cool city, which is Liupanshui City as the type locality of this new species enjoys the reputation of "China's Cool Capital". The noun is in apposition.

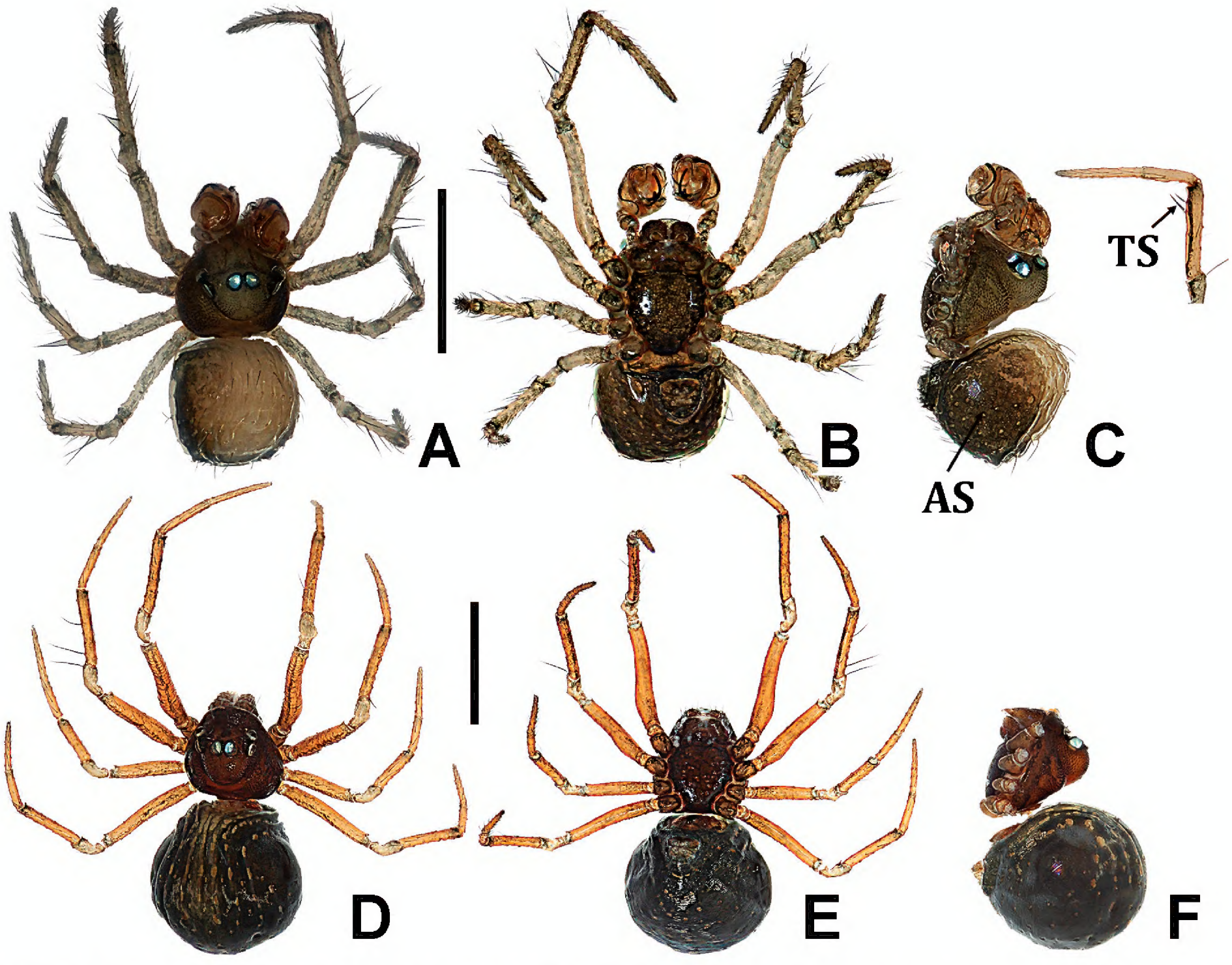

Figure 5. *Crassignatha liangdu* Wu & Lin, sp. nov. **A.** Male habitus, dorsal view; **B.** Ditto, ventral view; **C.** Ditto, lateral view; **D.** Female habitus, dorsal view; **E.** Ditto, ventral view; **F.** Ditto, lateral view. Scale bars: 0.50 mm (**A–F**).

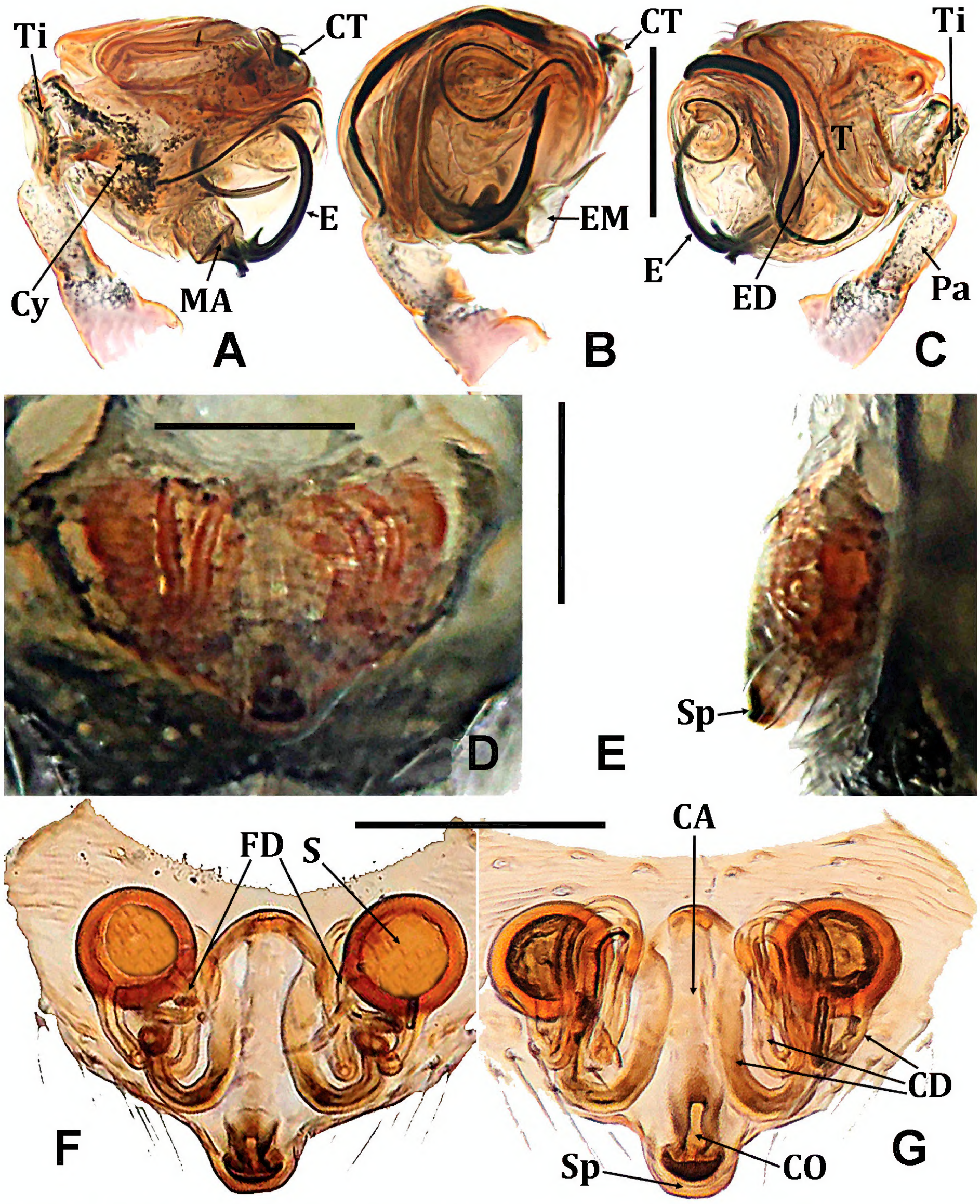

Figure 6. *Crassignatha liangdu* Wu & Lin, sp. nov. **A.** Male palp, prolateral view; **B.** Ditto, ventral view; **C.** Ditto, retrolateral view; **D.** Epigyne, ventral view; **E.** Ditto, lateral view; **F.** Vulva, dorsal view; **G.** Ditto, ventral view. Scale bars: 0.10 mm (**A–G**).

Diagnosis. The male of *Crassignatha* liangdu sp. nov. resembles those of *C. shiluensis*, *C. yamu*, and *C. panlong* sp. nov. in possessing a long, coiled embolus. It can be distinguished by the presence of a distinct basal embolic process and a broad embolic membrane, structures that are absent in the compared species (cf. Fig. 6A–C with Fig. 8A–C and Li et al. 2020: figs 27A, B, 35A–C). The female of *C. liangdu* sp. nov. is similar to those of *C. panlong* sp. nov., *C. si*, and *C. yamu* in the general configuration of the vulva and the course of the copulatory ducts. It differs in that the apex of the columnar atrium is level with the anterior margin of the spermatheca, whereas in the other species the apex is situated either above or below this margin (cf. Fig. 6F, G with Fig. 8F, G and Li et al. 2020: figs 31E, F, 35F, G).

Description. Male (holotype). Total length 0.74. Carapace 0.35 long, 0.31 wide, 0.33 high. Clypeus 0.13 high. Sternum 0.25 long, 0.20 wide. Abdomen 0.41 long, 0.39 wide, 0.41 high. Length of legs: I 1.06 (0.32, 0.13, 0.25, 0.15, 0.21); II 0.95 (0.29, 0.12, 0.21, 0.13, 0.20); III 0.79 (0.26, 0.10, 0.14, 0.10, 0.19); IV 0.83 (0.28, 0.09, 0.17, 0.10, 0.18).

Somatic characters (Fig. 5A–C). Prosoma rusty brown. Legs dark grey, with black pigmentation. Tibia II with two clasping spurs distoventrally. Opisthosoma darker laterally and ventrally than dorsally. Carapace nearly rounded, surface rough granular. Cephalic area elevated. Six eyes in three diads, PER slightly recurved, anterior lateral eyes protruded. Clypeal area slightly concaved. Labium fused to sternum. Sternum scutiform, with dense dark dotted pigmentation. Opisthosoma nearly globular dorsally, dorsal epidermis rugose, wrapped by weakly ossific scutum from laterally and posteriorly. Spinnerets with an annular shield.

Palp (Fig. 6A–C): relatively large, ~ ½ of carapace size. Tibia oblate, nearly equal to ¾ of patella in length. Cymbium wraps the bulb on prolaterally and posteroventrally, few bristles at distally, cymbial tooth conspicuous hooked-shaped. Tegulum smooth, swollen, the course of ejaculatory duct clearly visibel. Median apophysis small, sclerotized at distally. Embolic membrane broad, with a long sharp corner. Embolus long tubular, coiled into one loop, with a distinct basal process.

Female (one of the paratypes). Total length 1.00. Carapace 0.40 long, 0.36 wide, 0.40 high. Clypeus 0.13 high. Sternum 0.25 long, 0.25 wide. Abdomen 0.60 long, 0.62 wide, 0.64 high. Length of legs: I 1.48 (0.50, 0.13, 0.37, 0.23, 0.25); II 1.29 (0.42, 0.12, 0.31, 0.20, 0.24); III 0.96 (0.27, 0.11, 0.20, 0.18, 0.20); IV 1.21 (0.40, 0.12, 0.27, 0.19, 0.23).

Somatic characters (Fig. 5D–F). Prosoma chestnut brown, obvious ossified. Legs bright brown, with few black pigmentation on each segment. Opisthosoma almost all black, only scattered ossified, light brown sparkles on dorsal and anterior epidermis. Carapace pear-shaped, surface rough, granular. Cephalic area slightly elevated. ALE protruded, PER straight. Labium wider than long, fused to sternum. Sternum surface pitted, posteriorly truncated. Opisthosoma: rounded, spotted, and rugose dorsally and anteriorly. Spinnerets same as in male, with an annular shield.

Epigyne (Fig. 6D–G): epigynal area obviously sclerotized, internal structure faintly visible via the weakly ossified epidermis. Scape slightly protruded, equal length and width. Spermathecae globose, spacing by ~1.6× their diameter. Fertilization ducts originated from the posteromedial margin of spermathecas, and bent down and extend. Copulatory ducts extremely long and tortuous, connected with the posterolateral margin of spermathecae, folded upward and downward twice, and fused into a columnar atrium located between spermathecae. Copulatory opening large, opens longitudinally at the end of scape.

Distribution. China (Guizhou) (Fig. 13).

Crassignatha panlong Wu & Lin, sp. nov.

https://zoobank.org/83AD8554-51E1-4B58-AB0D-4BCB2CE96EF3

Figs 7, 8, 13

Type material. ***Holotype*** • ♂ (NHMSU Ar 175) and ***paratypes*** • 2♂ 5♀ (NHMSU Ar 176–182), **China:** Yunnan Prov., Kunming Ct., Panlong Dist., Xiaohe TWP., the entrance to Yanzi Cave (25.187943°N, 102.806825°E; elev. 2060 m), 27.VIII.2020, Y. Lin, Y. Li and S. Liu leg. 1♂ (NHMSU-YG162) and 1♀ (NHMSU-YG162) used for sequencing, same data as for preceding.

Etymology. The specific epithet derives from the name of the type locality; noun in apposition.

Diagnosis. Male of *Crassignatha panlong* sp. nov. is characterized by a linearly spiraled, elongate embolus, a feature shared only with *C. liangdu* sp. nov., *C. shiluensis*, and *C. yamu* (Fig. 8A–G). It differs from *C. shiluensis* and *C. yamu* by the presence of a distinct process at the base of the embolus, as opposed to a medially located process or its complete absence (cf. Fig. 8A with Li et al. 2020: figs 27A, 35A, B). It differs from *C. liangdu* sp. nov. by possessing a broad median apophysis and an indistinct embolic membrane (cf. Fig. 8A, B with Fig. 6A, B). Female of this new species shares *C. liangdu* sp. nov., *C. gudu*, *C. si*, and *C. yamu* with the presence of a columnar atrium formed by the fusion of the proximal sections of the copulatory ducts. It can be differentiated from these species by its longer columnar atrium, which extends beyond the anterior margin of the spermathecae, and/or by the less convoluted path of the copulatory ducts along the dorsal side of the spermathecae (cf. Fig. 8F, G with Fig. 6F, G and Li et al. 2020: figs 11E, F, 31E, F, 35E, F).

Description. Male (holotype). Total length 0.83. Carapace 0.36 long, 0.34 wide, 0.40 high. Clypeus 0.13 high. Sternum 0.23 long, 0.21 wide. Abdomen 0.47 long, 0.40 wide, 0.50 high. Length of legs: I 1.12 (0.32, 0.13, 0.28, 0.17, 0.22); II 0.95 (0.25, 0.12, 0.23, 0.13, 0.22); III 0.80 (0.22, 0.11, 0.15, 0.11, 0.21); IV 0.88 (0.28, 0.11, 0.20, 0.12, 0.17).

Somatic characters (Fig. 7A–C). Prosoma darkish-brown. Legs pale brown, with black pigmentation on each segment. Opisthosoma greyish black, dorsally lighter than laterally and ventrally. Carapace nearly rounded, surface coarse and granular, cervical groove obvious, cephalic area raised. Clypeal area concaved laterally. Six eyes in three diads, PRE recurved, ALE slightly protruded, PMEs spacing by ~ ¾ of their diameter. Entire mouthparts and sternum strongly sclerotized. Labium same long as wide, fused to sternum. Sternum scutiform, surface rough and uneven pitted, posteriorly truncated. Leg II with three large clasping spurs at the tibia ventral-distally, two long and one short. Opisthosoma short ovoid dorsally, nearly triangular laterally, smooth scutum wrapped abdomen at laterally and posteriorly. Abdominal epidermis rugose at anteriorly and dorsally, with various size of weakly ossified patches. One annular plates encircled spinnerets.

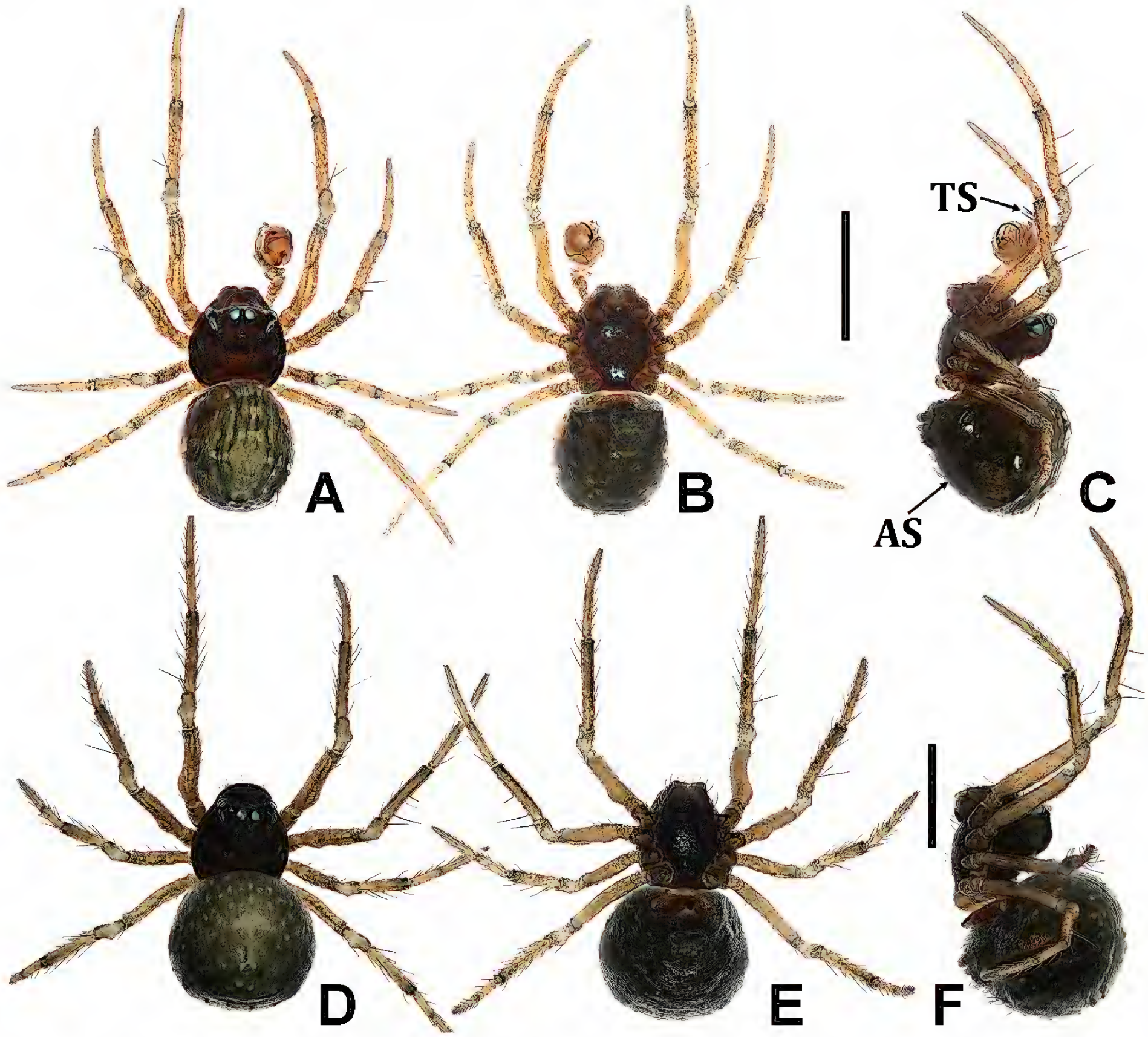

Figure 7. *Crassignatha panlong* Wu & Lin, sp. nov. **A.** Male habitus, dorsal view; **B.** Ditto, ventral view; **C.** Ditto, lateral view; **D.** Female habitus, dorsal view; **E.** Ditto, ventral view; **F.** Ditto, lateral view. Scale bars: 0.50 mm (**A–F**).

Palp (Fig. 8A–G): relatively small, ca. ~ one fifth of carapace size. Tibia oblate, same as long patella, wider than patella. Cymbium wrapped bulb at prolaterally, cymbial apex bears three short setae and a small hooked tooth (CT). Bulb translucent, internal convoluted ejaculatory duct clearly visible. Tegulum broad, smooth. Median apophysis oblate, with a small sclerotized corner distally. Embolic membrane narrow, undeveloped. Embolus starts at the base of median apophysis, convoluted a vertical coil suspended above the bulb, with the end gradually narrowing.

Female (one of the paratypes). Total length 1.10. Carapace 0.44 long, 0.58 wide, 0.41 high. Clypeus 0.12 high. Sternum 0.30 long, 0.26 wide. Abdomen 0.60 long, 0.72 wide, 0.68 high. Length of legs: I 1.49 (0.50, 0.13, 0.36, 0.23, 0.27); II 1.30 (0.43, 0.13, 0.30, 0.18, 0.26); III 1.02 (0.30, 0.11, 0.21, 0.16, 0.24); IV 1.18 (0.39, 0.13, 0.26, 0.17, 0.23).

Somatic characters (Fig. 7D–F). Entire coloration darker than in male. Prosoma darkish-brown and strongly sclerotized. Carapace nearly pear-shaped, surface coarse and granular. Cephalic area elevated, lower than in male. PER straight. Labium triangular, fused to the sternum. Legs deeper color than in male. Opisthosoma globose. Abdominal epidermis scattered with point-like speckles, dorsally more than laterals and ventrally.

Epigyne (Fig. 8D–G): epigynal area weakly sclerotized, slightly protruded, internal structure faintly visible. Scape extends beyond the epigastric furrow, distal end sclerotized. Spermatheca globose, separated by 1.7 × their diameter. Fertilization duct narrower than copulatory duct, originated from the posteromedial margin of spermatheca. Copulatory duct long, tortuous, connected to the posterior margin of spermatheca, extended downward and turn to the dorsum of spermatheca forming two reciprocating loops, and curved upward in an "s" shape toward vulva center, fused into a straight columnar atrium. The proximal end of columnar atrium forms into a copulatory opening, which opens at the end of scape.

Distribution. China (Yunnan) (Fig. 13).

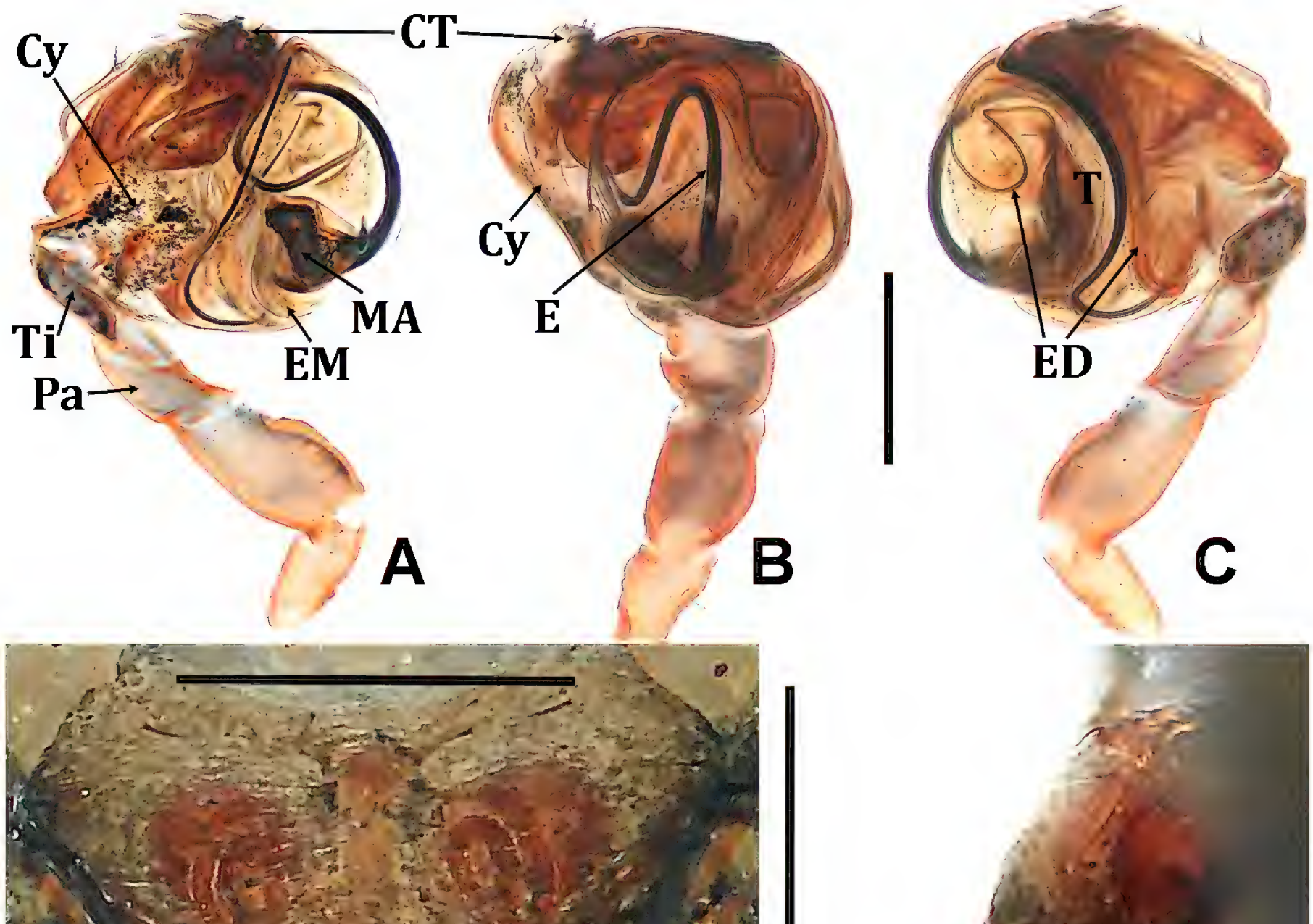

Figure 8. *Crassignatha panlong* Wu & Lin, sp. nov. **A.** Male palp, prolateral view; **B.** Ditto, ventral view; **C.** Ditto, retrolateral view; **D.** Epigyne, ventral view; **E.** Ditto, lateral view; **F.** Vulva, dorsal view; **G.** Ditto, ventral view. Scale bars: 0.10 mm (**A–G**).

Crassignatha qingxu Wu & Lin, sp. nov.

https://zoobank.org/8D01A181-C3B1-40E3-97B7-AE749AD3E090

Figs 9, 10, 13

Type material. ***Holotype*** • ♂ (NHMSU Ar 183) and ***paratypes*** • 2♂ 5♀ (NHMSU Ar 184–190), China: Guizhou Prov., Bijie Ct, Dafang Co., Yangchang TWP., Longgong Vill., the entrance to Qingxu Cave (27.103043°N, 105.669876°E; elev. 1476 m), 23.VIII.2020, Y. Lin et al. leg. 1♂ (NHMSU-YG170) and 1♀ (NHMSU-YG170) used for sequencing, same data as for preceding.

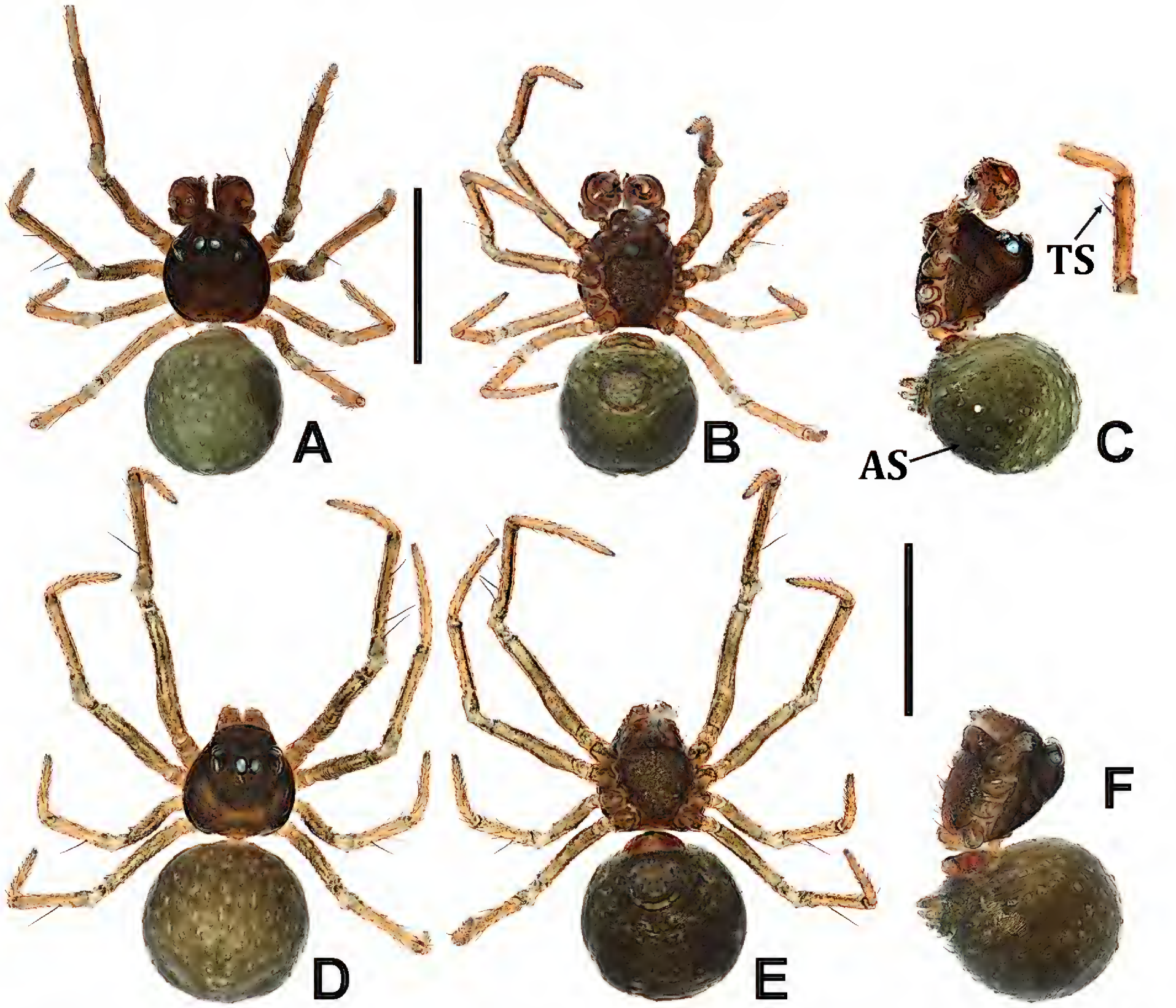

Figure 9. *Crassignatha qingxu* Wu & Lin, sp. nov. **A.** Male habitus, dorsal view; **B.** Ditto, ventral view; **C.** Ditto, lateral view; **D.** Female habitus, dorsal view; **E.** Ditto, ventral view; **F.** Ditto, lateral view. Scale bars: 0.50 mm (**A–F**).

Etymology. The specific epithet derives from the name of Qingxu Cave, which is a famous and huge cave in the local area as the type locality; noun in apposition.

Diagnosis. The male of *Crassignatha qingxu* sp. nov. is distinguished from all other congeners by the combination of a long, horn-like median apophysis and a furcate embolus (Fig. 10A, B). The female resembles those of *C. bangbie*, *C. ertou*, *C. nasalis*, *C. quanqu*, *C. thamphra*, and *C. yinzhi* in general vulval configuration. It can be differentiated by its distinctly larger spermathecae, inconspicuous fertilization ducts, and/or the less tortuous course of the copulatory ducts (cf. Fig. 10A–C with Li et al, 2020: figs 3F, G, 8F, G, 17E, F, 23D, E, 32F, G, and 37F, G).

Description. Male (holotype). Total length 0.84. Carapace 0.37 long, 0.34 wide, 0.35 high. Clypeus 0.15 high. Sternum 0.22 long, 0.21 wide. Abdomen 0.48 long, 0.43 wide, 0.47 high. Length of legs: I 1.18 (0.35, 0.12, 0.30, 0.17, 0.24); II 1.03 (0.33, 0.11, 0.24, 0.13, 0.22); III 0.81 (0.25, 0.10, 0.16, 0.11, 0.19); IV 0.92 (0.29, 0.10, 0.21, 0.12, 0.20).

Somatic characters (Fig. 9A–C). Prosoma sclerotized, coloration deeper than legs and opisthosoma. Carapace nearly rounded, surface granular. Cephalic area raised. Clypeal area concaved laterally. Ocular area slightly protruded, six eyes in three diads, PER recurved, lateral eyes contiguous, posterior median eyes spacing by ~¾ their diameter. Mouthparts compacted. Labium wider than long, fused to sternum. Sternum rouge and uneven, truncated posteriorly. Legs pale brown. Tibia II with two distal-ventrally clasping spurs. Opisthosoma globose, weakly scutum wraps abdomen at laterally and posteriorly, light spots scattered on abdomen dorsally and anteriorly. Spinnerets with an annular plate.

Palp (Fig. 10A–C): large, ~ ½ of carapace size. Patella slightly shorter than tibia. Cymbium wraps bulb only at prolaterally, cymbial apex bears short seta and a dentiform apophysis (CT). Tegulum swollen and smooth, internal ejaculatory duct distinctly obvious. Median apophysis sclerotized, presenting a long horn shape. Embolic membrane inconspicuous. Embolus short, rigid, extends from above the tegulum, and its end forms a nearly symmetrical fork.

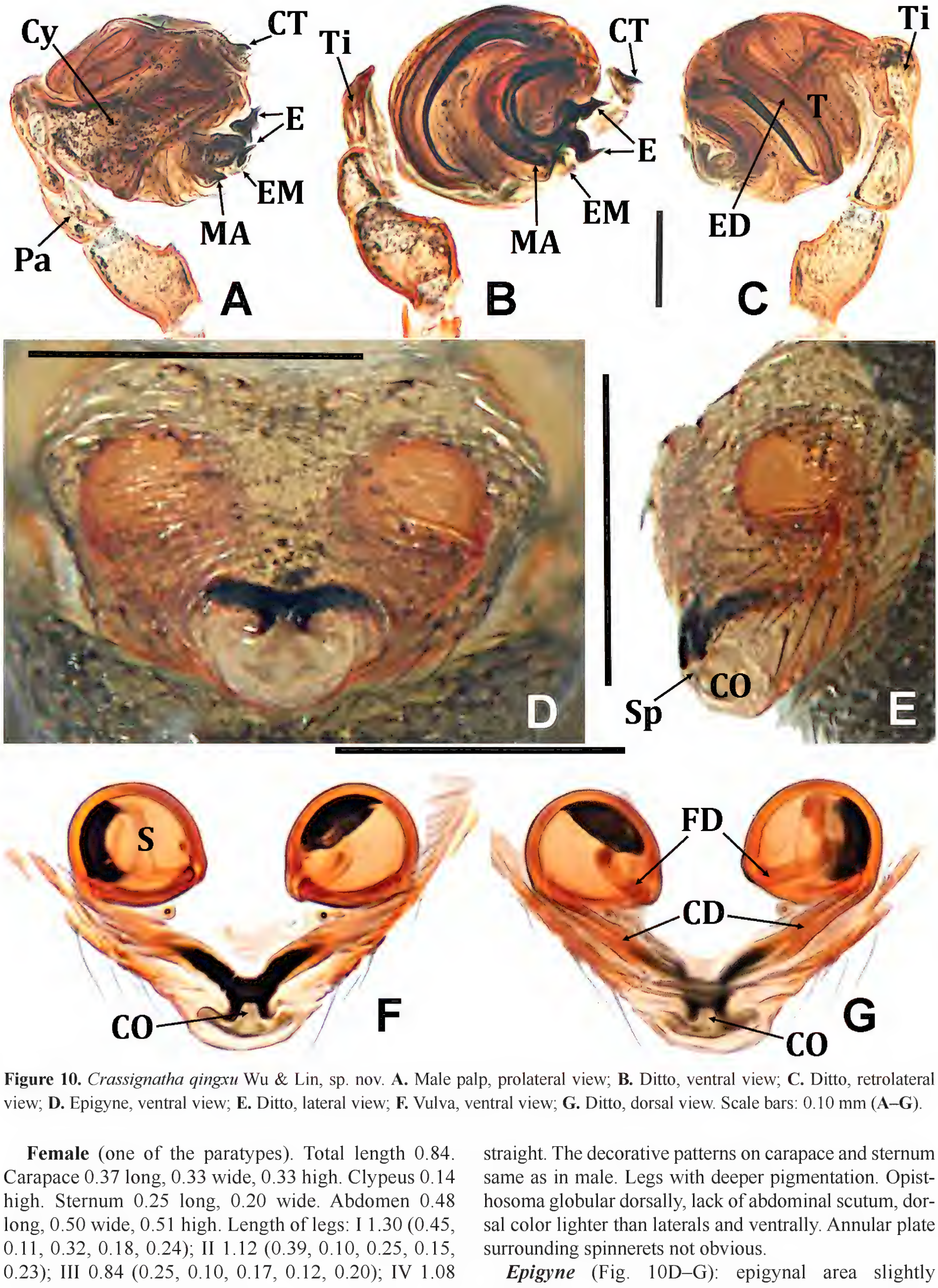

Figure 10. *Crassignatha qingxu* Wu & Lin, sp. nov. **A.** Male palp, prolateral view; **B.** Ditto, ventral view; **C.** Ditto, retrolateral view; **D.** Epigyne, ventral view; **E.** Ditto, lateral view; **F.** Vulva, ventral view; **G.** Ditto, dorsal view. Scale bars: 0.10 mm (**A–G**).

Female (one of the paratypes). Total length 0.84. Carapace 0.37 long, 0.33 wide, 0.33 high. Clypeus 0.14 high. Sternum 0.25 long, 0.20 wide. Abdomen 0.48 long, 0.50 wide, 0.51 high. Length of legs: I 1.30 (0.45, 0.11, 0.32, 0.18, 0.24); II 1.12 (0.39, 0.10, 0.25, 0.15, 0.23); III 0.84 (0.25, 0.10, 0.17, 0.12, 0.20); IV 1.08 (0.39, 0.11, 0.24, 0.14, 0.20).

Somatic characters (Fig. 9D–E). Body coloration same as in male. Carapace nearly pear-shaped. Cervical groove distinct. Cephalic area lower than in male. PER straight. The decorative patterns on carapace and sternum same as in male. Legs with deeper pigmentation. Opisthosoma globular dorsally, lack of abdominal scutum, dorsal color lighter than laterals and ventrally. Annular plate surrounding spinnerets not obvious.

Epigyne (Fig. 10D–G): epigynal area slightly bulged, internal structure faintly visible. Scape stubby. Spermathecae nearly spherical, separated by ~¾ their diameter. Fertilization duct unapparent, arises from the posteromedial margin of spermatheca, and then sharply

curves to spermathecal dorsum. The course of copulatory duct relatively simple, connected with the posterolateral margin of spermatheca, and extends to form a flat "V"-shaped structure. Copulatory ducts on both sides fused at the base of scape. Copulatory opening board, located at the end of scape.

Distribution. China (Guizhou) (Fig. 13).

Crassignatha shunani Y. Lin & S. Li, 2020

Figs 11, 12, 13

Type material. ***Holotype*** • ♂ (NHMSU Ar 073) and ***paratypes*** • 4♂ 49♀ (NHMSU Ar 074–126), **China:** Sichuan Prov., Luzhou Ct., Gulin Co., Jianzhu TWP., Wenyi Vill., the entrance of Dahei Cave (28.06134°N, 105.58015°E; elev. 852 m), 23.IV.2014, Y. Lin, H. Zhao and J. Wu leg.

Other material examined. • 2♂4♀ (NHMSU Ar 191–196), **China:** Guizhou Prov., Zunyi Ct., Honghuagang Distr., Shenxi TWP., Longjiang Vill., outside of the Guanniu Cave (27.613715°N, 106.969101°E; elev. 848 m), 23.VIII.2020, Y. Lin, Y. Li and S. Liu leg. 1♂ (NHMSU-YG157) and 1♀ (NHMSU-YG157) used for sequencing, same data as for preceding.

Diagnosis. *Crassignatha shunani* resembles *C. nantou* in possessing a long, spirally coiled embolus with a sharply pointed tip and in having copulatory ducts with disconnected bases (Fig. 12A–G). The male of *C. shunani* can be distinguished by the presence of a sharp cymbial tooth and the absence of a hooked process on the median apophysis (cf. Fig. 12A, B with Li et al. 2020: fig. 15A, B). Female differs from that of *C. nantou* in having more widely separated, ovoid spermathecae and a lower turning point of the copulatory ducts between them, as opposed to the more closely arranged, globose spermathecae and a higher turning point of copulatory duct in the latter species (cf. Fig. 12D–G with Li et al. 2020: fig. 15F, G).

Description. See Li et al. 2020: 110 and Figs 11A–F, 12A–G.

Distribution. China (Guizhou, Sichuan) (Fig. 13).

Remark. This study reports the first documented occurrence of *Crassignatha shunani* outside its type locality, representing a new provincial record for Guizhou.

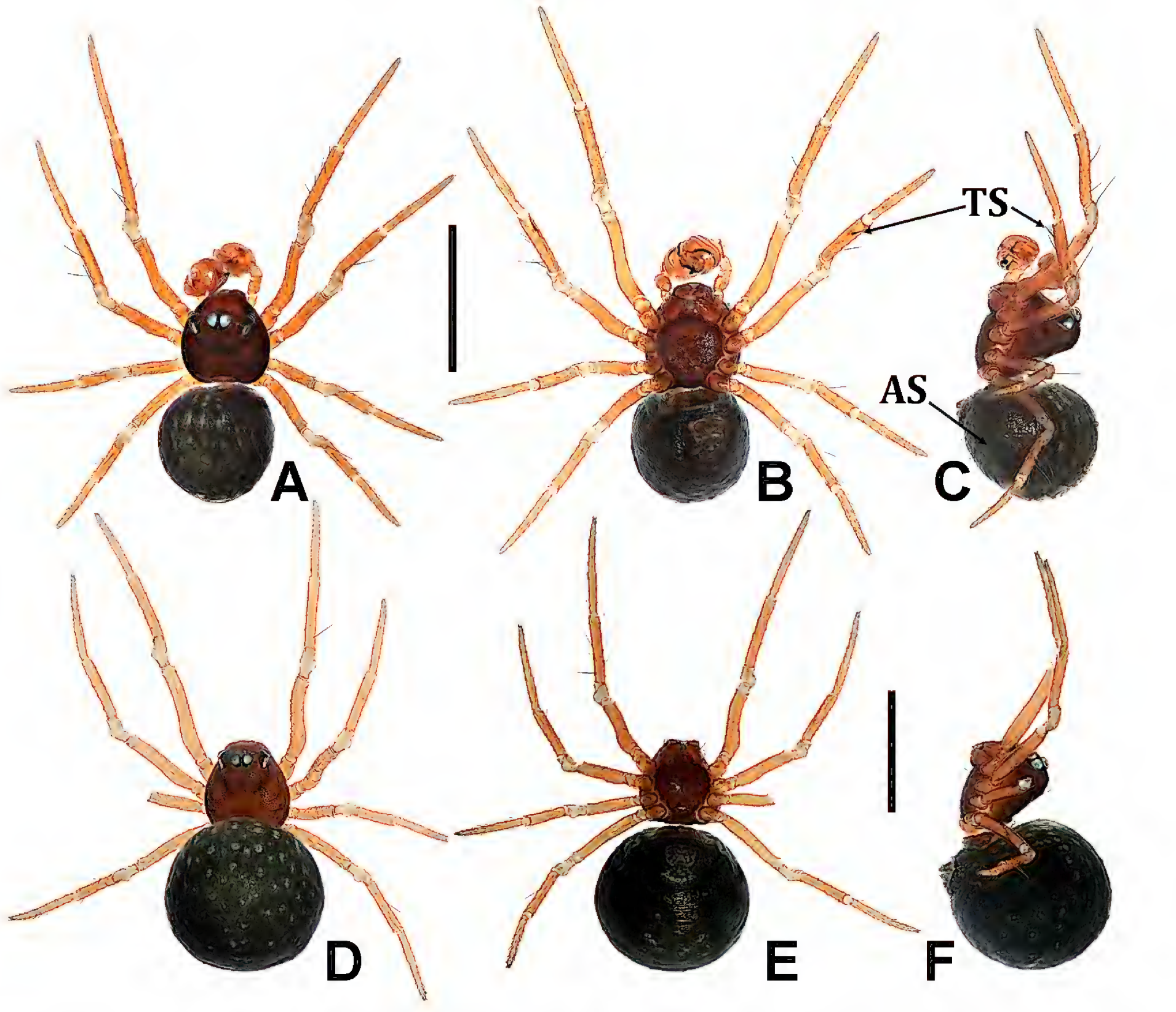

Figure 11. *Crassignatha shunani* Lin & **S.Q.** Li, 2020. **A.** Male habitus, dorsal view; **B.** Ditto, ventral view; **C.** Ditto, lateral view; **D.** Female habitus, dorsal view; **E.** Ditto, ventral view; **F.** Ditto, lateral view. Scale bars: 0.50 mm (**A–F**).

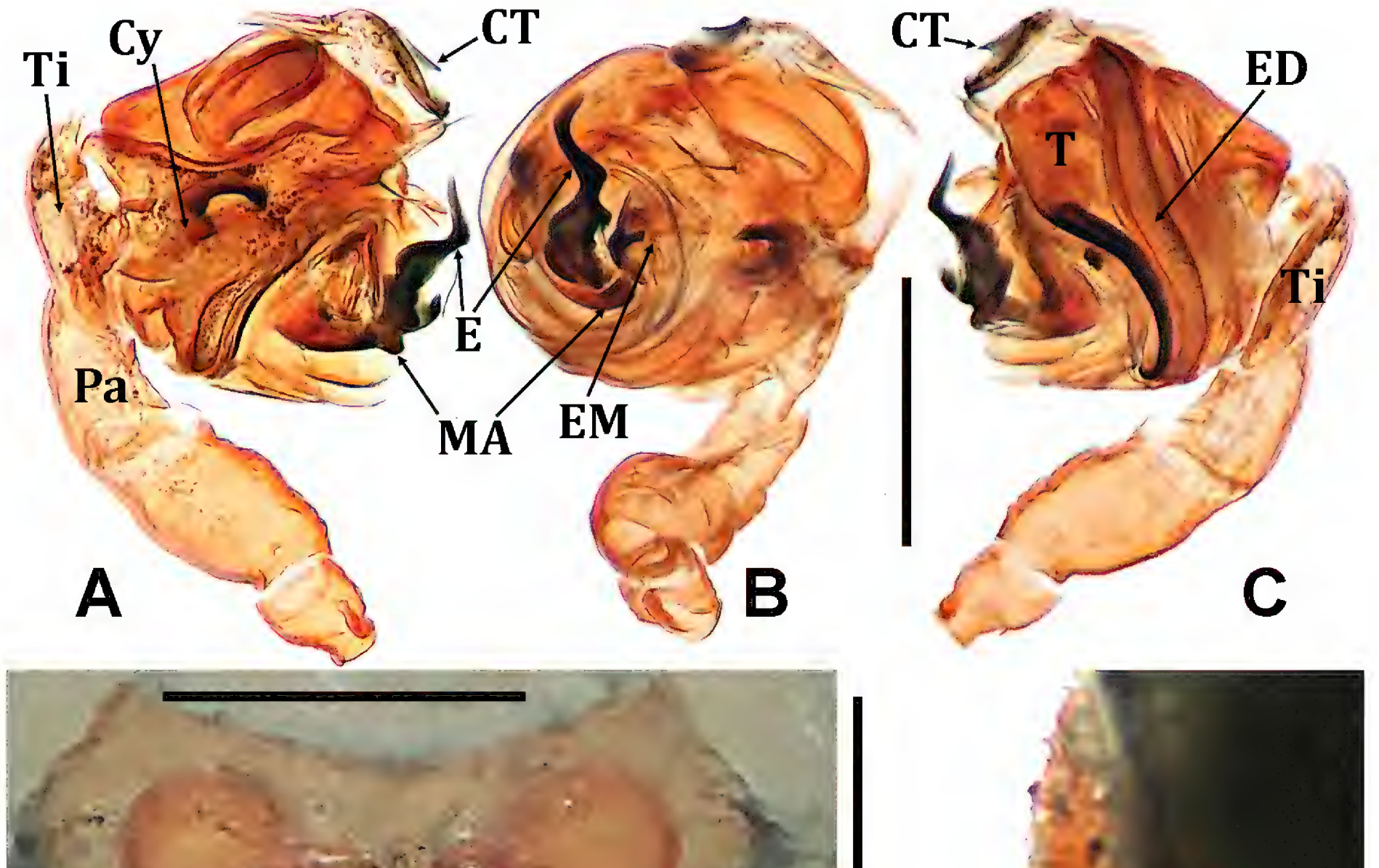

Figure 12. *Crassignatha shunani* Lin & S.Q. Li, 2020. **A.** Male palp, prolateral view; **B.** Ditto, ventral view; **C.** Ditto, retrolateral view; **D.** Epigyne, ventral view; **E.** Ditto, lateral view; **F.** Vulva, ventral view; **G.** Ditto, dorsal view. Scale bars: 0.10 mm (**A–G**).

Discussion

This study describes four new species of the spider genus *Crassignatha* from the Yunnan–Guizhou Plateau and provides an updated diagnosis for one previously recorded species. Phylogenetic analyses based on a multi-gene dataset strongly support the monophyly of *Crassignatha* and validate the status of the newly proposed species. Importantly, our results provide definitive molecular evidence for retaining *Crassignatha* within the family Symphytognathidae. This conclusion resolves a long-standing taxonomic uncertainty and aligns with recent phylogenomic findings based on ultraconserved element (UCE) data (Kulkarni et al. 2023).

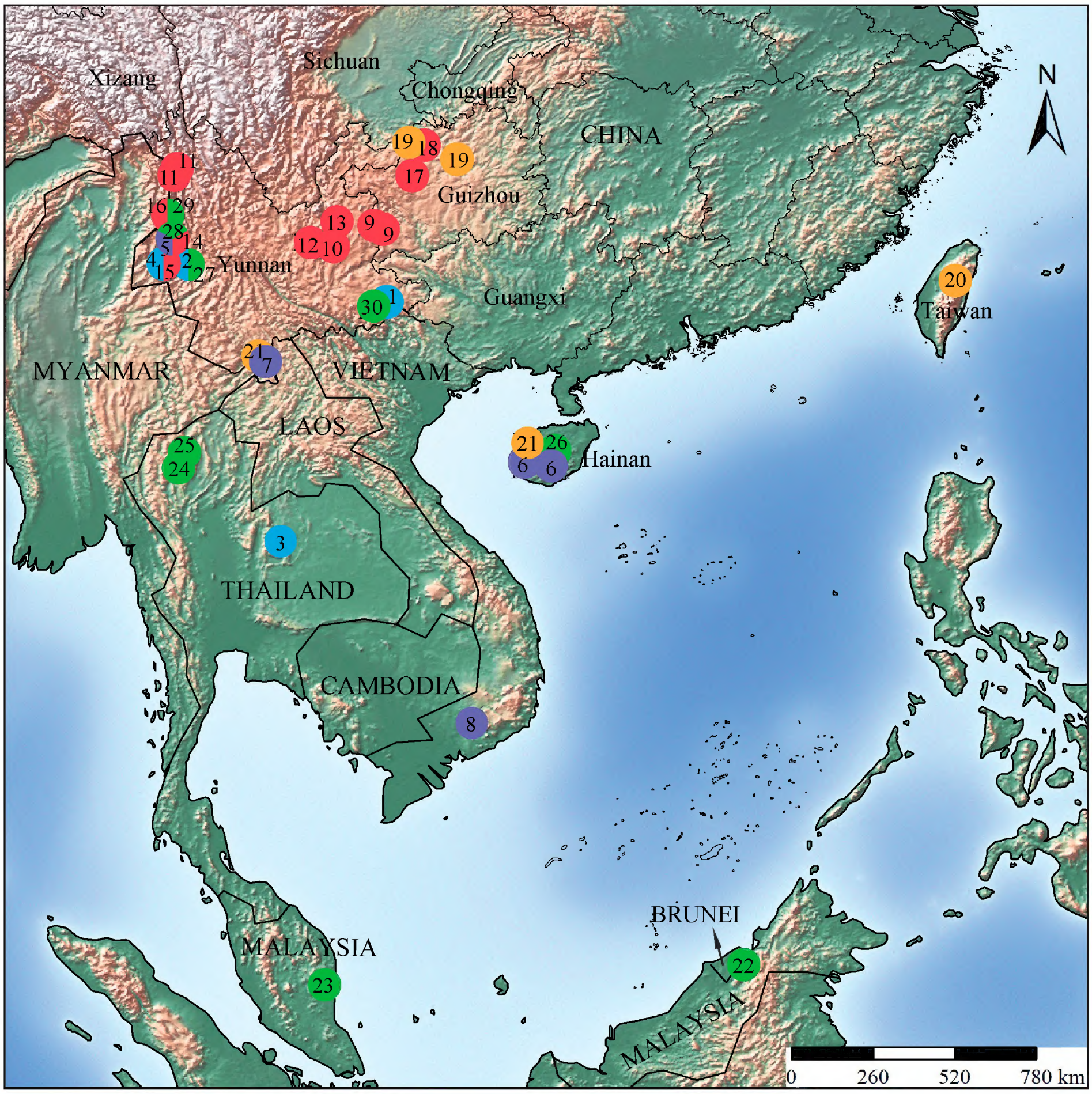

Figure 13. Distribution records of *Crassignatha* species in southern China and Southeast Asia. 1 *C. rostriformis*; 2 *C. bangbie*; 3 *C. thamphra*; 4 *C. gucheng*; 5 *C. baihua*; 6 *C. quadriventris*; 7 *C. mengla*; 8 *C. dongnai*; 9 *C. liangdu* sp. nov.; 10 *C. si*; 11 *C. yamu*; 12 *C. panlong* sp. nov.; 13 *C. hekou* sp. nov.; 14 *C. ertou*; 15 *C. yinzhi*; 16 *C. pianma*; 17 *C. qingxu* sp. nov.; 18 *C. nasalis*; 19 *C. shunani*; 20 *C. nantou*; 21 *C. shiluensis*; 22 *C. danaugirangensis*; 23 *C. haeneli*; 24 *C. seedam*; 25 *C. seeliam*; 26 *C. bicorniventris*; 27 *C. quanqu*; 28 *C. gudu*; 29 *C. changyan*; 30 *C. xichou*. Red, purple, blue, and yellow symbols correspond to branches in Figs 1, 2, whereas green symbols represent species not included in the phylogenetic analyses.

By integrating phylogenetic and geographic data (Fig. 13), our analyses reveal structured biogeographic patterns within *Crassignatha*: (1) early-diverging lineages (yellow symbols) occur broadly along the periphery of the genus's range, a pattern consistent with relictual distributions following early dispersal; (2) intermediate, transitional lineages (red symbols) are largely restricted to the karst core of the Yunnan–Guizhou Plateau, extending toward its margins, suggesting gradual range expansion from this center; (3) later-diverging lineages (purple and blue symbols) exhibit cross-regional, disjunct distributions. Notably, *C. shiluensis* (point 2) occurs in both Yunnan and Hainan, implying either transmarine dispersal or a past land-bridge connection; and (4) the distributions of the most recently diverged species (blue symbols) spatially overlap with those of the transitional lineages (red symbols), which may reflect microhabitat partitioning as a mechanism for reducing interspecific competition. Collectively, these patterns highlight the significant role of karst geomorphology in driving diversification and shaping the distribution of *Crassignatha*.

Our findings indicate that species of the genus *Crassignatha* have undergone range expansion and adaptive

radiation across the heterogeneous karst landscapes of the Yunnan–Guizhou Plateau. Phylogeographic patterns suggest that the phased uplift of the plateau and the evolution of major river systems, such as the Pearl River, served as key biogeographic barriers and corridors, respectively (Favre et al. 2015; Xing and Ree 2017). These processes likely facilitated eastward expansion while simultaneously promoting vicariance and allopatric speciation, as evidenced by the phylogenetic relationships among species from neighboring karst blocks. The observed distributions are consistent with two principal biogeographic mechanisms: (1) the complex karst topography likely provided a network of microrefugia during Pleistocene climatic oscillations, preserving relict populations (Manchester et al. 2009; Liu et al. 2022); and (2) the intrinsic fragmentation of limestone bedrock and associated cave systems has created persistent dispersal barriers, driving allopatric speciation and restricting contemporary gene flow among populations (Sajid et al. 2021; Weng et al. 2022; Liu et al. 2023; Rodríguez-Flores et al. 2025). Ecologically, although not obligate troglobites, *Crassignatha* species show a pronounced preference for mesic, dark microhabitats, including deep cave zones, sheltered rock overhangs, and thick leaf litter within karst forests (Miller et al. 2009). Consequently, the availability of suitable limestone substrates fundamentally constrains their distributions and reinforces patterns of regional endemism. Overall, the interplay between prolonged geographic isolation and ecological adaptation to karst habitats appears to have been central to the remarkable diversification of *Crassignatha* within this biodiversity hotspot.

Despite these advances, our study highlights several limitations that warrant attention in future research. First, persistent sampling gaps in Guizhou and adjacent karst regions likely result in an underestimation of species richness; more systematic cave surveys are needed to clarify patterns of troglomorphic evolution and to inform conservation priorities. Second, the scarcity of specimens limited molecular data availability for several species, leaving their delimitation reliant on morphology alone. This underscores the need for additional collections of molecular material to enable integrative taxonomic validation. Finally, expanded sampling of outgroup taxa across Symphytognathidae is essential to resolve deeper phylogenetic relationships within the family.

Acknowledgments

We thank Jeremy Miller (Naturalis Biodiversity Center, Leiden, Netherlands) and an anonymous reviewer for their constructive comments. We also extend our sincere gratitude to the subject editor, Dr. Danilo Harms (Leibniz Institute for the Analysis of Biodiversity Change, Hamburg, Germany), for his editorial guidance. We are grateful to Dr. Yun-chun Li (China West Normal University, Nanchong) and to Mr. Y. Li, Ms. Y. He, and Mr. S. Liu for their assistance with field collection. This research was funded by the National Natural Science Foundation of China (Grants NSFC-31972870 and 31750002).

References

Balczun C, Bunse A, Nowrousian M, Korbel A, Glanz S, Kück U (2005) DNA macroarray and real-time PCR analysis of two nuclear photosystem I mutants from *Chlamydomonas reinhardtii* reveal down-regulation of Lhcb genes but different regulation of Lhca genes[J]. Biochimica et Biophysica Acta (BBA) - Biochimica et Biophysica Acta. Gene Structure and Expression 1732(1–3): 62–68. https://doi.org/10.1016/j.bbaexp.2005.11.006

Brescovit AD, Cizauskas I (2025) Description of three new species of *Anapistula* Gertsch, 1941 from caves, with new distribution records for Brazilian *Symphytognatha carstica* Brescovit, Álvares & Lopes, 2004 (Araneae: Symphytognathidae). Arachnology 20(3): 428–438. https://doi.org/10.13156/arac.2024.20.3.9

Cardoso P, Scharff N (2009) First record of the spider family Symphytognathidae in Europe and description of *Anapistula ataecina* sp. n. (Araneae). Zootaxa 2246(1): 46–57. https://doi.org/10.11646/zootaxa.2246.1.4

Colgan DJ, McLauchlan A, Wilson GS, Livingston SP, Edgecombe GD, Macaranas J, Cassis G, Gray MR (1998) Histone H3 and U2 snRNA DNA sequences and arthropod molecular evolution. Australian Journal of Zoology 46(5): 419–437. https://doi.org/10.1071/ZO98048

Dunlop JA, Penney D, Jekel D (2023) A summary list of fossil spiders and their relatives. In World Spider Catalog. Natural History Museum Bern. http://wsc.nmbe.ch [version 23.5, accessed on 1 Oct. 2025]

Esri (2020) ArcGIS Desktop 10.8. Redlands, CA: Environmental Systems Research Institute. https://www.esri.com/

Favre A, Päckert M, Pauls SU, Jähnig SC, Uhl D, Michalak I, Muellner-Riehl AN (2015) The role of the uplift of the Qinghai-Tibetan Plateau for the evolution of Tibetan biotas. Biological Reviews of the Cambridge Philosophical Society 90(1): 236–253. https://doi.org/10.1111/brv.12107

Forster RR, Platnick NI (1977) A review of the spider family Symphytognathidae (Arachnida, Araneae). American Museum Novitates 2619: 1–29.

Giribet G, Carranza S, Baguñà J, Riutort M, Ribera C (1996) First molecular evidence for the existence of a Tardigrada + Arthropoda clade. Molecular Biology and Evolution 13(1): 76–84. https://doi.org/10.1093/oxfordjournals.molbev.a025573

Hormiga G, Arnedo M, Gillespie RG (2003) Speciation on a Conveyor Belt: Sequential Colonization of the Hawaiian Islands by Orsonwelles spiders (Araneae, Linyphiidae). Systematic Biology 52(1): 70–88. https://doi.org/10.1080/10635150390132786

Katoh K, Standley DM (2013) MAFFT (Version 7.450). https://mafft.cbrc.jp/alignment/software/

Khmelik VV, Kozub D, Glazunov A (2006) Helicon Focus 3.10.3. Helicon Focus Helicon SoftHelicon Soft. [accessed on 20 June 2025]

Kulkarni S, Wood HM, Hormiga G (2023) Advances in the reconstruction of the spider tree of life: A roadmap for spider systematics and comparative studies. Cladistics: The International Journal of the Willi Hennig Society 39(6): 479–532. https://doi.org/10.1111/cla.12557

Kumar S, Stecher G, Suleski M, Sanderford M, Sharma S, Tamura K (2024) MEGA12: Molecular evolutionary genetic analysis version 12.0.10 [Computer software]. Pennsylvania State University. https://www.megasoftware.net

Letunic I, Bork P (2021) Interactive Tree of Life (iTOL) v5: An online tool for phylogenetic tree display and annotation. Nucleic Acids Research 49(W1): 293–296. https://doi.org/10.1093/nar/gkab301

Li Y, Lin Y, Li S (2020) A review of *Crassignatha* (Araneae, Symphytognathidae). ZooKeys 988: 63–128. https://doi.org/10.3897/zookeys.988.56188

Li Y, Li S, Lin Y (2021) Taxonomic study on fourteen symphytognathid species from Asia (Araneae, Symphytognathidae). ZooKeys 1072: 1–47. https://doi.org/10.3897/zookeys.1072.67935

Lin Y, Li S (2009) First described *Patu* spiders (Araneae, Symphytognathidae) from Asia. Zootaxa 2154(1): 47–68. https://doi.org/10.11646/zootaxa.2154.1.3

Liu Y, Wang S, Xu S, Fabel DM, Stuart F, Rodés Á, Zhang X, Luo W (2022) New chronological constraints on the Plio-Pleistocene uplift of the Guizhou Plateau, SE margin of the Tibetan Plateau. Quaternary Geochronology 67: 101237. https://doi.org/10.1016/j.quageo.2021.101237

Liu S, Zhou C, Lin Y (2023) New Insights into the Variation and Admixture of the Cave-Dwelling Spider *Trogloneta yunnanensis* in South China Karst. Animals 13(7): 1244. https://doi.org/10.3390/ani13071244

Lopardo L, Hormiga G (2015) Out of the twilight zone: Phylogeny and evolutionary morphology of the orb-weaving spider family Mysmenidae, with a focus on spinneret spigot morphology in symphytognathoids (Araneae, Araneoidea). Zoological Journal of the Linnean Society 173(3): 527–786. https://doi.org/10.1111/zoj.12199

Mammola S, Michalik P, Hebets EA, Isaia M (2017) Record breaking achievements by spiders and the scientists who study them. PeerJ 5(e3972): e3972. https://doi.org/10.7717/peerj.3972

Manchester SR, Chen ZD, Lu AM, Uemura K (2009) Eastern Asian endemic seed plant genera and their paleogeographic history throughout the Northern Hemisphere. Journal of Systematics and Evolution 47(1): 1–42. https://doi.org/10.1111/j.1759-6831.2009.00001.x

Marusik YM, Lehtinen PT (2003) Synaphridae Wunderlich, 1986 (Aranei: Araneoidea), a new family status, with a description of a new species from Turkmenistan. Arthropoda Selecta 11: 143–152.

Miller JA, Griswold C, Yin C (2009) The symphytognathoid spiders of the Gaoligongshan, Yunnan, China (Araneae: Araneoidea): Systematics and diversity of micro-orbweavers. ZooKeys 11: 9–195. https://doi.org/10.3897/zookeys.11.160

Miller JA, Schilthuizen M, Lilliendahl Burmester J, van der Graaf L, Merckx V, Jocque M, Kessler PJA, Fayle TM, Breeschoten T, Broeren R, Bouman R, Chua WJ, Feijen F, Fermont T, Groen K, Groen M, Kil NJC, de Laat HA, Moerland MS, Moncoquet C, Panjang E, Philip AJ, Roca-Eriksen R, Rooduijn B, van Santen M, Swakman V, Evans MN, Evans LJ, Love K, Joscelyne SH, Tober AV, Wilson HF, Ambu LN, Goossens B (2014) Dispatch from the field: Ecology of ground-web-building spiders with description of a new species (Araneae, Symphytognathidae). Biodiversity Data Journal 2(e1076): 1–13. https://doi.org/10.3897/BDJ.2.e1076

Nguyen L, Schmidt H, von Haeseler A, Minh B (2015) IQ-TREE: A fast and effective stochastic algorithm for estimating maximum-likelihood phylogenies. Molecular Biology and Evolution 32(1): 268–274. https://doi.org/10.1093/molbev/msu300

Palumbi SR, Martin RA, Romano S, McMillan WO, Stice SL (1991) The simple fool's guide to PCR, Version 2.0. University of Hawaii, Honolulu. Privately published, compiled by S. Palumbi.

Rambaut A, Drummond AJ, Xie D, Baele G, Suchard MA (2018) Posterior summarization in Bayesian phylogenetics using Tracer 1.7. Systematic Biology 67(5): 901–904. https://doi.org/10.1093/sysbio/syy032

Rivera-Quiroz FA, Petcharad B, Miller JA (2021) First records and three new species of the family Symphytognathidae (Arachnida, Araneae) from Thailand, and the circumscription of the genus *Crassignatha* Wunderlich, 1995. ZooKeys 1012: 21–53. https://doi.org/10.3897/zookeys.1012.57047

Rix MG, Harvey MS, Roberts JD (2008) Molecular phylogenetics of the spider family Micropholcommatidae (Arachnida: Araneae) using nuclear rRNA genes (18S and 28S). Molecular Phylogenetics and Evolution 46(3): 1031–1048. https://doi.org/10.1016/j.ympev.2007.11.001

Rodríguez-Flores PC, Derkarabetian S, Isaia M, Mammola S, Giribet G (2025) Population genomics of a cave-dwelling Arachnid (Palpigradi, Eukoeneniidae) from the South-Western Italian Alps. Zoologica Scripta 54(6): 1–13. https://doi.org/10.1111/zsc.12739

Ronquist F, Teslenko M, van der Mark P, Ayres D, Darling A, Höhna S, Larget B, Liu L, Suchard M, Huelsenbeck J (2012) MrBayes 3.2: Efficient Bayesian phylogenetic inference and model choice across a large model space. Systematic Biology 61(3): 539–542. https://doi.org/10.1093/sysbio/sys029

Sajid A, Khan MZ, Zhang W (2021) Impact of cave fragmentation on subterranean biodiversity: A global synthesis. Subterranean Biology 38: 112–135. https://doi.org/10.3897/subtbiol.38.67541

Shinkai E (2009) Two new species of the genera *Wendilgarda* and *Patu* from Japan (Araneae: Theridiosomatidae and Symphytognathidae). In: Ono H (Ed.) The spiders of Japan with keys to the families and genera and illustrations of the species. Tokai University Press, Kanagawa, 75–77.

Simon C, Frati F, Beckenbach A, Beckenbach A, Crespi B, Liu H, Flook P (1994) Evolution, Weighting, and Phylogenetic Utility of Mitochondrial Gene Sequences and a Compilation of Conserved Polymerase Chain Reaction Primers. Annals of the Entomological Society of America 87(6): 651–701. https://doi.org/10.1093/aesa/87.6.651

Weng Y, McShe W, Diao YX, Yang HB, Zhang XF, Gu BJ, Bu HL, Wang F (2022) The incursion of free-ranging dogs into protected areas: A spatio-temporal analysis in a network of giant panda reserves. Biological Conservation 265: 109423. https://doi.org/10.1016/j.biocon.2021.109423

WSC (2025) World Spider Catalog. Version 26. Natural History Museum Bern. http://wsc.nmbe.ch [accessed on 1 Oct. 2025]

Wunderlich J (1986) Spinnenfauna gestern und heute: Fossile Spinnen in Bernstein und ihre heute lebenden Verwandten. Quelle & Meyer, Wiesbaden, 283 pp.

Wunderlich J (1995) Drei bisher unbekannte Arten und Gattungen der Familie Anapidae (s.l.) aus Süd-Afrika, Brasilien und Malaysia (Arachnida: Araneae) [Three previously unknown species and genera of the family Anapidae (s.l.) from South Africa, Brazil, and Malaysia (Arachnida: Araneae)]. Beiträge zur Araneologie 4(1994): 543–551.

Wunderlich J (2004) The fossil spiders of the family Anapidae s. l. (Aeaneae) in Baltic, Dominican and Mexican amber and their extant relatives, with the description of the new subfamily Comarominae. Beiträge zur Araneologie 3: 1020–1111.

Xing YW, Ree RH (2017) Uplift-driven diversification in the Hengduan Mountains, a temperate biodiversity hotspot. Proceedings of the National Academy of Sciences of the United States of America 114(17): E3444–E3451. https://doi.org/10.1073/pnas.1616063114

Zhang Q, Lin Y (2023) Phylogenetic placement of eight poorly known spiders of *Microdipoena* (Araneae, Mysmenidae), with descriptions of five new species. ZooKeys 1175: 333–373. https://doi.org/10.3897/zookeys.1175.90920

Zhang D, Gao F, Jakovlić I, Zou H, Zhang J, Li WX, Wang GT (2020) PhyloSuite: An integrated and scalable desktop platform for streamlined molecular sequence data management and evolutionary phylogenetics studies. Molecular Ecology Resources 20(1): 348–355. https://doi.org/10.1111/1755-0998.13096

Supplementary material 1

Appendix A

Author: Haihong Wu
Data type: xlsx
Explanation note: Uncorrected genetic pairwise distances (below the diagonal) and standard errors (above the diagonal) for a partial fragment of COI among 21 *Crassignatha* species discussed in this study.
Copyright notice: This dataset is made available under the Open Database License (http://opendatacommons.org/licenses/odbl/1.0/). The Open Database License (ODbL) is a license agreement intended to allow users to freely share, modify, and use this Dataset while maintaining this same freedom for others, provided that the original source and author(s) are credited.
Link: https://doi.org/10.3897/zse.102.165834.suppl1